AR-001-658

DEPARTMENT OF DEFENCE

DEFENCE SCIENCE AND TECHNOLOGY ORGANISATION

ELECTRONICS RESEARCH LABORATORY

TECHNICAL REPORT

ERL-0074-TR

THE EFFECT OF SCINTILLATIONS ON TRANSIONOSPHERIC COMMUNICATIONS

D.G. Singleton

S U M M A R Y

Consideration is given to the bearing ionospheric scintillation has on the design and on the evaluation of the performance of satellite communication links. Emphasis is placed on establishing a design parameter of universal application. The cumulative amplitude distribution function (cdf), which has found application in this regard, is shown experimentally to be well represented by the Nakagami m-distribution at all scintillation levels. However, the cdf is demonstrated to be strictly valid only for amplitude modulated signals of short duration. Autocorrelation, power spectra and level crossing techniques are investigated in an effort to establish a design parameter more universally applicable than the cdf. A quantity message reliability, is defined which removes the short duration restriction inherent in the cdf. A formula for message reliability is developed which allows it to be evaluated for any fade margin and message length, given the scintillation index and the half width of the autocorrelogram of the scintillating channel. A design chart, embodying this information, is also illustrated.

POSTAL ADDRESS: Chief Superintendent, Electronics Research Laboratory, Box 2151, G.P.O., Adelaide, South Australia, 5001.

TABLE OF CONTENTS

LIST OF FIGURES

12. The distributions for the scintillations shown in figure 7(a)

13. The reliability factor (A) as a function of normalised message length $(r/\tau_{0.5})$ for several values of $\chi_0\sqrt{m}$

1. INTRODUCTION

Communication links involving transionospheric propagation are subject to disruption due to ionospheric scintillation(ref.1). The scintillation takes the form of random fluctuations in both the amplitude and the phase of the received signal. This effect is most marked in the VHF/UHF region of the electromagnetic spectrum but it is also evident at SHF and above(ref.2). The effect is due to perturbations introduced into a steady incident wave by irregularities of electron density which exist mainly in the F-layer of the ionosphere(ref.1). The occurrence of these irregularities has been studied for a number of years(ref.3) and their global occurrence morphology has been documented to such an extent that this morphology is now amenable to successful modelling(ref.4,5,6). However, this report is concerned not with the occurrence morphology but rather with the nature of the degradation of a communications channel caused by the presence of scintillations.

Scintillations cause both enhancements and fading of the signal about a median level as well as random fluctuations in phase. When scintillation fades occur which exceed the fade margin built into a communications link, the performance of the link will be degraded. The degree of degradation will depend on how far the signal fades relative to the fade margin, the duration of the fade, the type of modulation employed and the criteria of acceptability for the channel. In this report discussion of these factors will be illustrated with an analysis of UHF data obtained with the aid of MARISAT II(ref.7).

The report commences in the next Section by considering the source of the data employed. This is followed in Section 3 by theoretical and experimental considerations of the effect scintillations have on signals of short duration. Section 4 extends these considerations to signals of longer duration. Finally, the conclusions reached are summarized and discussed in Section 5.

2. THE DATA

The scintillation data analysed in the following Sections was obtained by observing MARISAT II at Manus Island (147.37^{o}E, 2.04^{o}S)(ref.7). MARISAT II is at synchronous altitude over the equator at 176.5^{o}E and hence was viewed a little north of east and at an elevation of about 56^{o} from Manus Island. The carrier at 256.550 MHz, known as the Fleet Broadcast Channel, which operates with time division multiplexed phase shift keyed modulation at 1200 bits/s was monitored with a receiver of high dynamic range. An IF bandwidth of 7 kHz was used while a post-detection bandwidth of 5 Hz was employed. The receiver's AGC voltage was digitized with 6 bit sampling and the digital data was recorded on magnetic tape. At least one calibration was carried out each day, which allowed the digitized AGC data to be converted in the subsequent processing to equivalent signal power (dBm) at the antenna.

In digitizing the data a sample rate of 10 samples/s was used. This corresponds to a Nyquist frequency of 5 Hz. Since the scintillation frequencies of interest are less than 1 Hz, the resultant oversampling of the analog information affords some protection against aliasing. This protection was further enhanced by the action of the post-detection filter.

It is planned to provide the receiving equipment with the capability of recording the bit error rate detected in the phase shift keyed modulation of the satellite's transmissions. The bit error rate is expected to be sensitive to the signal's phase stability as well as its power stability, whereas the AGC measurements are a measure of the signal power stability only. However, no bit error rate data were available at the time this report was written.

3. SMALL DURATION SIGNALS

In this Section consideration will be given to the effect scintillations have on communications channels which are carrying signals of short duration, e.g. digital data at rates of the order of kilobits per second and higher. Consideration of the effects scintillations have on signals of relatively long duration, e.g. as in voice communications, will be deferred to Section 4.

3.1 Theory

In order to quantify the fluctuations in the amplitude (R) of a scintillating signal, a quantity called the scintillation index (S_4) can be defined as follows(ref.8).

$$S_4 = [\{\overline{R^4} - (\overline{R^2})^2\} / (\overline{R^2})^2]^{\frac{1}{2}} \quad (1)$$

This index proves to be a convenient measure of scintillation activity when the observation of scintillations is used as a technique for studying ionospheric irregularities. This is because the index can be related directly to the properties of the irregularities(ref.8,9). However, in the engineering of communication circuits employing transionospheric propagation, a more system oriented measure is needed, such as the probability of communication being lost due to scintillation effects.

For most communication systems, the "outage" probability can be defined in terms of the probability of the signal level falling below some designated value. For example, in the interval T for the scintillating signal illustrated in figure 1, the outage probability $U(\chi_0)$ at a margin of χ_0 relative to the median level, is given by

$$U(\chi_0) = \sum_{t=0}^{T} \delta t_f / T$$

On the other hand, the probability of the signal being above the margin χ_0 is

$$P(\chi_0) = \sum_{t=0}^{T} \delta t_s / T = 1 - U(\chi_0) \quad (2)$$

The signal fluctuates at the receiver because it is a random superposition of random vectorial elements. Nakagami(ref.10) has investigated such systems extensively and has shown that the probability distribution p(R) of the resultant signal amplitude (R) is represented by

$$p(R) = \frac{2m^m R^{2m-1}}{\Gamma(m)(\overline{R^2})^2} \exp\left(\frac{-mR^2}{\overline{R^2}}\right)$$

This is known as the m-distribution and it can be demonstrated that

$$m = 1/S_4^2 \quad (3)$$

It is worth noting that the m-distribution reduces to the Rayleigh distribution in the special case where m = 1. The Rayleigh distribution is the classical result for the distribution expected from a superposition of random vectors. Strictly it applies only to the case where there is no steady signal component, whereas the m-distribution encompasses both this possibility and that where there is a background signal.

Defining the signal level χ as

$$\chi = 10 \log_{10} (R^2/\overline{R^2})$$

the m-distribution in terms of signal level becomes

$$p'(\chi) = \frac{2m^m}{M\,\Gamma(m)} \exp[\,m\{2\chi/M - \exp(2\chi/M)\}\,] \tag{4}$$

where

$$M = 20 \log_{10} e = 8.686 \tag{5}$$

It follows that the probability of the signal level falling below some specified level (i.e. the outage probability) is

$$U(\chi_0) = \int_{-\infty}^{\chi_0} p'(\chi)\,d\chi = \int_{-\infty}^{\chi_0} \frac{2m^m}{M\,\Gamma(m)} \exp[\,m\{2\chi/M - \exp(2\chi/M)\}\,]\,d\chi$$

Similarly the probability of the signal being above the margin χ_0 is

$$P(\chi_0) = \int_{\chi_0}^{\infty} p'(\chi)\,d\chi = \int_{\chi_0}^{\infty} \frac{2m^m}{M\,\Gamma(m)} \exp[\,m\{2\chi/M - \exp(2\chi/M)\}\,]\,d\chi \tag{6}$$

$P(\chi_0)$ has become known as the cumulative amplitude probability distribution function or cdf(ref.11) and is plotted (as a percentage) for a series of values of m in figure 2. Here the signal levels (χ_0) are referred to the median level at which χ_0 is set zero.

For amplitude modulated signals of sufficiently short duration, the outage rate will closely approximate the instantaneous outage probability $U(\chi_0)$. Hence for amplitude modulated signals with bit rates in excess of about 1 kbits/s, the bit error rate (BER) will equal $U(\chi_0)$. That is, for such signals

$$\text{BER} = 100 - \text{cdf} \tag{7}$$

Bits may be lost from signals which involve phase shift keying either because of amplitude scintillation or because of phase scintillation. Hence for such phase modulated signals

$$\text{BER} \geqslant 100 - \text{cdf} \tag{8}$$

Because of the greater instrumental difficulties involved in their observation, little data is available on phase scintillation. However, the random-phase screen theory of scintillation(ref.12) shows that the spatial scale of the amplitude fluctuations is always less than the spatial scale of

TABLE 1. PARAMETERS FOR THE PERIODS OF SCINTILLATION ANALYSED

Year	Day	Start L.T.	S_4	m	$\tau_{0.5}$ (s)	f_c (Hz)	p
1976	237	0030	0.20	24.9	5.5	0.025	2 to 3
1976	236	2330	0.37	7.2	3.35	0.04	3 to 4
1976	236	2300	0.65	2.3	2.6	0.05	4 to 5
1976	236	1930	0.86	1.3	7.25	(0.02)	3 to 4
1976	236	2000	1.08	0.9	2.9	(0.02)	4 to 5

the associated phase fluctuations in the diffraction pattern produced by a screen(ref.13,14). Further, the differences in the scale sizes increases with the r.m.s. phase deviation and hence with scintillation index. Since the amplitude and the phase scintillations are both the result of the movement of the diffraction pattern across the observing point, it follows that the phase fluctuations are generally slower than the associated amplitude fluctuations, the disparity increasing with increasing scintillation index. This being the case, amplitude scintillations will be the predominant factor in determining the bit error rate for phase modulated signals especially when the scintillation index is large. This conclusion is apparently borne out by observation(ref.15).

3.2 Experimental verification

Because of the connection between BER and cdf noted in the previous Section, it is important to verify that the m-distribution is a valid representation of the instantaneous probability distribution of the signal amplitude. While verifications of this type have been carried out for values of m near unity(ref.11,16), the data described in Section 2 allow the validity of the m-distribution representation to be evaluated for a whole range of values of m.

Figure 3(a) shows the analog representation of the signal strength fluctuations during a period of 30 min commencing on 0030 hours L.T. on day 237 of 1976. During this period the application of equation (1) to the digital data yields a scintillation index of 0.20 which corresponds to an m value of 24.9 (equation (3)). The cdf values at 1 dB intervals of χ_0 about the median were also calculated from the digital data for this period using equation (2). The points obtained are plotted on figure 3(b). The line on figure 3(b) is obtained from equation (6). The m-distribution representation of the cdf (equation (6)) obviously fits the experimental data well at this value of m.

Figures 4 to 7 inclusive display similar information to that just described for figure 3, except the scintillations involved are characterised by scintillation indices of 0.37 to 1.08 or alternatively by m values of 7.2 to 0.9 (vide Table 1). In each case the m-distribution representation of the cdf (equation (6)) is seen to give a good representation of the experimental cdf values. Any discrepencies which occur do so at the largest or smallest values of χ_0 investigated, where the statistics involved in the evaluation of equation (2) are likely to be inaccurate because of the small numbers of events encountered. Therefore, the m-distribution representation of the cdf (equation (6)) may be taken as a valid representation of the actual cdf

values observed regardless of the value of m. A similar conclusion can be reached with regards to the estimation of bit error rates (equations (7) and (8)) given the value of S_4 or m.

4. LONG DURATION SIGNALS

The cumulative amplitude probability distribution function (cdf), described in Section 3.1, besides giving information on the probability of reception of short period signals propagating in a scintillating channel, also describes the amplitudes of the fades which affect signals of longer period (e.g. > 0.1 s) when transmitted via such a channel. However, the full statistical description of the effect of scintillations on long duration signals also requires information on the fading rate. Such information can be obtained by employing either spectral techniques or level-crossing techniques. These techniques will be considered in the following Sections.

4.1 The autocorrelation function

The autocorrelation function is a way of characterizing the rate of the scintillation fading. It is defined in terms of the signal intensity I for a time lag τ as follows.

$$\rho(\tau) = \langle I(t)\ I(t+\tau)\rangle / \langle I^2(t)\rangle$$

Here $\langle\ \rangle$ denotes the average over the interval examined (T).

Autocorrelograms for lags (τ) up to 50 s have been calculated for each of the 30 min periods analysed for cdf (figures 3 to 7). These appear as part (a) of each of the figures 8 to 12 inclusive. In each case increasing the lag τ causes the autocorrelation coefficient to fall from unity at $\tau = 0$, to zero correlation at a value of τ which varies from correlogram to correlogram. Further increases of τ sees the correlation coefficient take on negative values and then return to oscillate about a coefficient of zero. The time lag at which the correlation coefficient falls to 0.5 ($\tau_{0.5}$) was measured off each correlogram and this measure of the correlogram width was tabulated in Table 1.

Perusal of the values of $\tau_{0.5}$ in Table 1 shows that they can vary by a factor of three. They are not obviously dependent on the value of scintillation index (or m) but are a measure of the average period of the fluctuations of amplitude of the scintillating signals.

4.2 Power spectra

The power spectrum of a scintillating signal is a graphic way of depicting the frequency structure of its amplitude fluctuations. The spectrum is the Fourier transform of the autocorrelation function(ref.17) and hence is represented by

$$F(f) = \frac{1}{2\pi} \int_{-\infty}^{\infty} e^{2\pi i f\tau}\ \rho(\tau)\ d\tau$$

Power spectra for each of the half-hour samples listed in Table 1 have been computed and these are displayed as part (b) of each of the figures 8 to 12 inclusive. The horizontal arm of each of the three small crosses on these diagrams indicate the frequency resolution applicable to that part of the spectrum, while the vertical arm indicates the magnitude of the statistical noise expected(ref.17).

In general the spectral shape consists of a relatively flat low-frequency spectrum and a high frequency roll-off of substantially constant slope. The break point between the low and the high frequency slopes, called the cut-off frequency (f_c), is a measure of the bandwidth of the spectrum. It is more clearly defined for those cases with a scintillation index of less than 0.7 (figures 8(b), 9(b) and 10(b)) as compared to those cases with higher scintillation index (figures 11(b) and 12(b)). Estimates of the cut-off frequency are tabulated in Table 1. The figures for the last two samples are enclosed in brackets to indicate their tentative nature which results from the ill-defined break points involved.

Because the power spectrum is the Fourier transform of the autocorrelation function, the bandwidth of the spectrum would be expected to be inversely proportional to the width of the autocorrelation function. Indeed $\tau_{0.5}\, f_c$ is substancially constant for the first four samples listed in Table 1. On the basis of this relationship a cut-off frequency of about 0.05 Hz would be expected for the sample commencing at 2000 hours on day 236. This value lies midway between the low and the high frequency regions of constant slope (figure 12(b)) and may well be a more realistic measure of the bandwidth than the 0.02 Hz quoted in Table 1.

As illustrated in figures 8 to 12 inclusive, the high frequency roll-off in each of the spectra involves a slope proportional to f^{-p}, where p has a value between 2 and 5. This result is consistent with observations at other frequencies(ref.18). It is obvious from the value of p for each of the spectra (Table 1) that p tends to increase with scintillation index.

4.3 Fade durations

The techniques described in Sections 4.1 and 4.2, i.e. the autocorrelation and the power spectrum techniques, undoubtedly give an insight into the temporal aspects of the full statistical description of a scintillating communications channel. However, they do little to alleviate the difficulties which the communications circuit designer experiences in this area. Consequently, in this and the next Section, level-crossing techniques will be investigated to ascertain whether they can offer a solution to the problem.

The level-crossing techniques seek to analyse the scintillating channel by gathering statistics on the distribution of fades at various signal levels. In the first of these techniques to be described, the durations of fades below a particular level are determined and tabulated against time interval. The levels or fade margins considered range, in 2 dB steps, from -2 dB to -10 dB relative to the median. From these tabulations, the cumulative distributions of fade duration for each fade margin can be constructed(ref.16). In parts (c) of each of figures 8 to 12 inclusive, these cumulative distributions of fade duration are plotted for the signal samples listed in Table 1. The points on these diagrams represent the results for each of the time interval cells chosen. The broken line curves were drawn freehand through the points to give an indication of the likely smoothed distribution for each fade margin. The distributions show that both the number of fade margins affected and the number of fades below each margin increase with scintillation index. This is the expected result as the overall depth of fading increase with scintillation index.

The S-like shape of the cumulative distribution curves suggests that the corresponding simple distribution curves should be bell shaped. Replotting the data as simple distributions verifies this. However, the number of events per cell are such that there is considerable statistical noise and no firm conclusion can be reached as to the nature of the distributions (e.g. whether they are normal distributions or not). One thing is clear however, the fade duration distributions are contained between upper and lower limits. The lower limit is about 0.2 to 0.5 s and the upper limit lies between 3 and 10 s. There is some variability of the limits within each set of distribution curves. Generally speaking however, the larger the fade margin, the closer the limits. Also the distribution limits vary

from one sample to another. For example, both the upper and lower limits of the distributions for the sample of scintillations represented in figure 11(c) are noticeably higher than those for the other samples illustrated. This is not unexpected as the correlogram width for this sample is larger than for the others (Table 1).

While this type of presentation of the level-crossing data gives some insight into the temporal character of the scintillation statistics, it, like the autocorrelation and spectral approaches, is not easily related to the engineering problem. However, the next Section shows how this data, expressed in a slightly different way, can yield answers to the engineer's queries.

4.4 Message reliability

Refering to figure 1, it can be seen that for a signal of a particular duration to be reliably received by a system with a fade margin corresponding to χ_0, it must fit completely within an enhancement of the signal above χ_0 (e.g. within δt_s). Consequently, a quantity, message reliability $R(r, \chi_0)$, can be defined(ref.16) for a sample of scintillations of duration T seconds, as the ratio of the number of time intervals or messages (of duration r seconds) that completely fit within those signal enhancements, which exceed a specified signal level (χ_0), to the total number which could fit within T. That is

$$R(r,\chi_0) = \frac{\sum_0^T \lfloor \delta t_s/r \rfloor}{T/r} \qquad (9)$$

where the operator $\lfloor\ \rfloor$ produces truncation of any fractional part of its argument. Equation (i) can be rewritten as

$$R(r,\chi_0) = \frac{\sum_0^T r\lfloor \delta t_s/r \rfloor}{T}$$

Now as r approaches zero $\sum_0^T r\lfloor \delta t_s/r \rfloor$ approaches $\sum_0^T \delta t_s$. Recalling equation (2), it is clear that in the limit r = 0, $R(r, \chi_0)$ is equivalent to the cumulative amplitude probability distribution function $P(\chi_0)$. That is the cdf is the ultimate message reliability which can be obtained with a scintillating channel for a particular fade margin and this is achieved only with very short duration signals. If message reliability could be given some analytical expression, it would provide a means of estimating the increase in fade margin which is required by a message of finite duration over the value specified by the cdf for infinitesimal signals, in order to maintain a given probability of perfect reception.

4.4.1 Experimental results

The second level-crossing technique which has been applied to the scintillation data involves evaluating message reliability for message lengths (r) ranging from 0.1 s to 100 s and for fade margins (χ_0) ranging from -2 dB to -10 dB. The results of this analysis for the data samples listed in Table 1 are illustrated in part (d) of each of the figures 8 to 12 inclusive. Here message reliabilities (as percentages) are plotted against message length.

In these figures the family of points for each sample of scintillation and for each value of χ_0 appear to lie along a well defined curve. These curves, which are substantially horizontal for the smaller message lengths, roll-off to smaller message reliabilities at the longer message lengths. A check shows that for each of the curves, the message reliability found for the smallest message length examined (0.1 s) corresponds to the cdf value expected for the values of m and χ_0 involved (figure 2). Indeed, the departure from the cdf value does not become appreciable until the message length exceeds about 5 s.

Increasing the scintillation index results in both a general decrease in message reliability for any fade margin and also increases the number of fade margins so affected. Also comparison of figure 11(d) with figures 10(d) and 12(d) shows that, while they each represent severe scintillation, the high message length roll-off of message reliability occurs at a larger value of r in figure 11(d) than in the other two figures. This is consistent with the larger autocorrelogram width ($\tau_{0.5}$) for the data sample from which figure 11(d) is produced compared to the values of $\tau_{0.5}$ for the data samples corresponding to the other two figures (Table 1). These are, of course, results which are expected on the basis of the discussions of Sections 4.1 to 4.3 inclusive. They reaffirm the suggestion made earlier that a statistic, which purports to fully represent the effects of scintillation on a communications channel, must take both the amplitude and the time dependencies into account.

4.4.2 Empirical theory

If message reliability is to be developed as a quantity which is useful in the engineering of scintillating communications channels, it is necessary to give it analytic expression. This Section will develop such an expression in a semi-empirical way.

The probability of the disturbed signal being at a level χ ($p'(\chi)$) is known (equation (4)). The message reliability depends on this probability and also on the probability of the disturbed signal at or above a level χ_0 remaining at or above that level for a time r. If this latter probability is called the abiding probability $a(\chi_0, r)$, then the message reliability can be written

$$R(\chi_0, r_0) = \int_{\chi_0}^{\infty} \int_{r_0}^{T} p'(\chi)\, a(\chi_0, r)\, dr d\chi$$

$$= \int_{\chi_0}^{\infty} p'(\chi)\, d\chi \int_{r_0}^{T} a(\chi_0, r)\, dr$$

Using equation (6) this becomes

$$R(\chi_0, r_0) = P(\chi_0) \int_{r_0}^{T} a(\chi_0, r)\, dr$$

or

$$R(\chi_0, r_0) = P(\chi_0)\, A(\chi_0, r_0) \tag{10}$$

That is, the message reliability is equal to the cdf times a reliability factor $A(\chi_0, r_0)$ where

$$A(\chi_0, r_0) = \int_{r_0}^{T} a(\chi_0, r)\, dr$$

It has been demonstrated experimentally (Section 4.4.1) that $A(\chi_0, r_0)$ is equal to or less than unity. It approaches unity as r_0 approaches zero and its departure from unity is only appreciable for values of r_0 in excess of about 5 s.

If the data of each part (d) of figures 8 to 12 inclusive are replotted with linear message length scales, the groups of experimental points fall along straight lines of negative slope which intercept the message reliability axis at the appropriate cdf values. That is

$$\log_{10} R(\chi_0, r_0) = \log_{10} P(\chi_0) - kr_0$$

or

$$R(\chi_0, r_0) = P(\chi_0)\, 10^{-kr_0} \tag{11}$$

It is then found that a log-linear plot of χ_0 versus k yields a straight line of negative slope for each of the data samples represented in figures 8 to 12 inclusive. Hence

$$\log_{10} \chi_0 = \log_{10} L - ck$$

where L is the intercept on the χ_0 axis. This can be rewritten as

$$10^{k} = (L/\chi_0)^{1/c}$$

which when combined with equation (11) yields

$$R(\chi_0, r_0) = P(\chi_0)\, (L/\chi_0)^{-r_0/c} \tag{12}$$

Since the quantity L is related to signal level, it is most likely to be dependent on scintillation index. Indeed it is found that, for the five scintillation samples listed in Table 1, L is directly proportional to scintillation index, the relationship being

$$L = -17.3\ S_4 \tag{13}$$

Since $2M = 17.37$ (equation (5)) and $m = 1/S_4^2$ (equation (3)), equation (13) can be conveniently restated as

$$L = -2M/\sqrt{m} \tag{14}$$

In a similar way, since c is related to message length r_0, c is most likely to be related to the time dependence of the scintillation. It is found that for the five samples of scintillation illustrated, c is directly proportional to $\tau_{0.5}$, the relationship being

$$c = 10.4\ \tau_{0.5} \tag{15}$$

Combination of equations (12), (14) and (15) gives finally

$$R(\chi_0, r_0) = P(\chi_0)(-2M/\sqrt{m}\ \chi_0)^{-0.096\ r_0/\tau_{0.5}} \tag{16}$$

or

$$R(\chi_0, r_0) = (-2M/\sqrt{m}\ \chi_0)^{-0.096\ r_0/\tau_{0.5}} \int_{r_0}^{\infty} \frac{2m^m}{M\ \Gamma(m)} \exp[m\{2\chi/M - \exp(2\chi/m)\}]\ d\chi \tag{17}$$

Comparing equation (16) with equation (10), it is seen that

$$A(\chi_0, r_0) = \int_{r_0}^{T} a(\chi_0, r)\ dr = (-2M/\sqrt{m}\ \chi_0)^{-0.096\ r_0/\tau_{0.5}} \tag{18}$$

Consequently, the abiding probability $a(\chi_0, r)$ is given by

$$a(\chi_0, r) = \frac{0.096}{\tau_{0.5}} \log(-2M/\sqrt{m}\ \chi_0)(-2M/\sqrt{m}\ \chi_0)^{-0.096\ r/\tau_{0.5}}$$

To further demonstrate the validity of equation (17), it was used to simulate the variation of message reliability with message length for the conditions pertaining to each of the families of experimental points plotted on parts (d) of each of the figures 8 to 12 inclusive. The broken line curves on these figures are the result of these simulations and, as can be seen, good agreement is obtained with the experimental points.

4.4.3 Circuit design chart

The above discussion indicates that message reliability is a convenient single parameter for characterizing the effects of scintillations on a transionospheric communications channel. For signals of short duration, message reliability is equivalent to the cdf which is a measure of circuit performance already in common use (ref.11,16,18). An algorithm for the computation of the cdf can be based on equation (6), while for most communications circuit design purposes, the graph presented as figure 2 would provide cdf values to sufficient accuracy.

For signals of duration greater than about a second, message reliability takes on values less than the cdf value, the reliability factor $A(\chi_0, r_0)$ (equation (18)) being the appropriate multiplying factor. From equation (16) this is

$$A(\chi_0, r_0) = R(\chi_0, r_0)/P(\chi_0) = (-2M/\sqrt{m}\,\chi_0)^{-0.096\, r_0/\tau_{0.5}} \qquad (19)$$

Equation (19) could be used as the basis for the construction of an algorithm for the calculation of the reliability factor. An algorithm for the complete computation of message reliability ($R(\chi_0, r_0)$) would be based on both equations (6) and (19).

Examination of the form of equation (19) suggests that a plot of $A(\chi_0, r_0)$ versus $r/\tau_{0.5}$ and parametric in $\chi_0\sqrt{m}$ would provide a useful chart for circuit design purposes. Figure 13 is such a diagram. Note

$$A(\chi_0, r_0) = 1 \text{ for } \chi_0\sqrt{m} = -2M = -17.37$$

$$A(\chi_0, r_0) < 1 \text{ for } \chi_0\sqrt{m} < -2M$$

while values of χ_0 and m which make $\chi_0\sqrt{m} > -2M$ are physically incompatable.

Figures 2 and 13 allow message reliability to be determined quickly for particular fade margins χ_0 and message lengths r_0 given a knowledge of m (or scintillation index) and $\tau_{0.5}$.

5. DISCUSSION AND CONCLUSIONS

In order to facilitate the design and to evaluate the performance of satellite communication links which are subject to scintillation, it is necessary to characterize scintillation in a manner different to that which has been found valuable when using scintillation for the study of ionospheric irregularities. The engineer designing a satellite communications link, needs to know what fraction of the time communications are likely to be disrupted and how, by suitably choosing certain parameters of the system, he can minimise this loss. The cumulative amplitude probability distribution function (cdf) has been used as such a design parameter. However, it has been shown that this is appropriate only for signals of short duration (< 1 s) and then strictly only for amplitude modulated signals.

If signals with durations of a second or more are to be catered for, the cdf is no longer a suitable design parameter and account has to be taken of the temporal character of the scintillations. The quantity message reliability which is defined above, provides to be a parameter which is suitable in this regard. It is valid for signals of all durations and includes the cdf estimate as a special case when the signal duration is small (< 1 s). Further, message

reliability has been shown to be a meaningful statistic for all levels of scintillation activity. However, like the cdf, it is strictly valid only for amplitude modulated signals, though the approximation involved for other types of modulation improves with increasing message duration.

The relationship between message reliability and cdf has been investigated in a semi-empirical way using UHF scintillation data. The formula so developed allows message reliability to be evaluated for any fade margin (χ_o) and message length (r) given the m factor and the half width of the autocorrelogram ($\tau_{0.5}$) appropriate to the scintillating channel. A design chart has been produced which gives expression to this formula and allows message reliability to be evaluated readily in terms of $r/\tau_{0.5}$ and $\chi_o\sqrt{m}$.

The data used in the analysis leading to the formulation of the message reliability expression applies to one carrier frequency and one location. The formula's validity for other frequencies and locations obviously need to be evaluated. Also bit error rate measurements obtained from phase modulated signals are needed to further evaluate the usefulness of the cdf and message reliability concepts for such signals.

6. ACKNOWLEDGEMENTS

The author would like to thank Mr N.F. Barkam and the technical staff of Communications Technology Group, Advanced Engineering Laboratory for providing the scintillation data whose analysis is presented in this report.

REFERENCES

No.	Author	Title
1	Getmantsev, G.G. and Eroukhimov, L.M.	"Radio Star and Satellite Scintillations". Annals of the IQSY, Vol.5, p229, 1969
2	Taur, R.R.	"Ionospheric Scintillation at Frequencies Above 1 GHz". COMSAT Tech. Rev., Vol.4, p461, 1974
3	Herman, J.R.	"Spread F and Ionospheric F-region Irregularities". Rev. Of Geophys., Vol.4, p255, 1966
4	Fremouw, E.J. and Bates, H.F.	"Worldwide Behaviour of Average VHF-UHF Scintillations". Radio Sci., Vol.6, p863, 1971
5	Fremouw, E.J. and Rino, C.L.	"An Empirical Model for Average F-Layer Scintillation at VHF-UHF". Radio Sci., Vol.8, p213, 1973
6	Singleton, D.G.	"An Improved Ionospheric Irregularity Model". ERL-0046-TR, November 1978
7	Barkam, N.F.	"UHF Equatorial Scintillation Fading Experiment". Proc. TTCP STP-7 Subgroup S Meeting November 1975, Vol.2, p53, 1976
8	Briggs, B.H. and Parkin, I.A.	"On the Variation of Radio Star and Satellite Scintillations with Zenith Angle". J. Atmosph. Terr. Phys., Vol.25, p339, 1963
9	Singleton, D.G.	"The Effect of Irregularity Shape on Radio Star and Satellite Scintillations". J. Atmosph. Terr. Phys., Vol.32, p315, 1970
10	Nakagami, M.	"Statistical Methods in Radio-Wave Propagation". Edited by W.C. Hoffman (Pergamon Press New York, 1960) pp3-36
11	Whitney, H.E., Aarons, J., Allen, R.S. and Seeman, D.	"Estimation of the Cumulative Amplitude Probability Distribution Function of Ionospheric Scintillations". Radio Sci., Vol.7, p1095, 1972
12	Ratcliffe, J.A.	"Some Aspects of Diffraction Theory And their Application to the Ionosphere". Rep. Progress in Phys., Vol.19, p188, 1956
13	Mercier, R.P.	"Diffraction by a Screen Causing Large Random Phase Fluctuations". Proc. Cam. Phil. Soc., Vol.58, p382, 1962
14	Bramley, E.N. and Young, M.	"Diffraction by a Deeply Modulated Random-Phase Screen". Proc. IEE, Vol.114, p553, 1967

No.	Author	Title
15	Blank, A.	"Burst-Error Characteristics of the Equatorial Transionospheric Channel". Proc. National Telecommunications Conference, San Diego, December 1974, p304
16	Whitney, H.E. and Basu, S.	"The Effect of Ionospheric Scintillation On VHF-UHF Satellite Communications". Radio Sci., Vol.12, p123, 1977
17	Singleton, D.G.	"Power Spectra of Ionospheric Scintillations". J. Atmos. Terr. Phys., Vol.36, p113, 1974
18	Singleton, D.G.	"Predicting Transionospheric Propagation Conditions". ERL-0049-TR (In preparation)

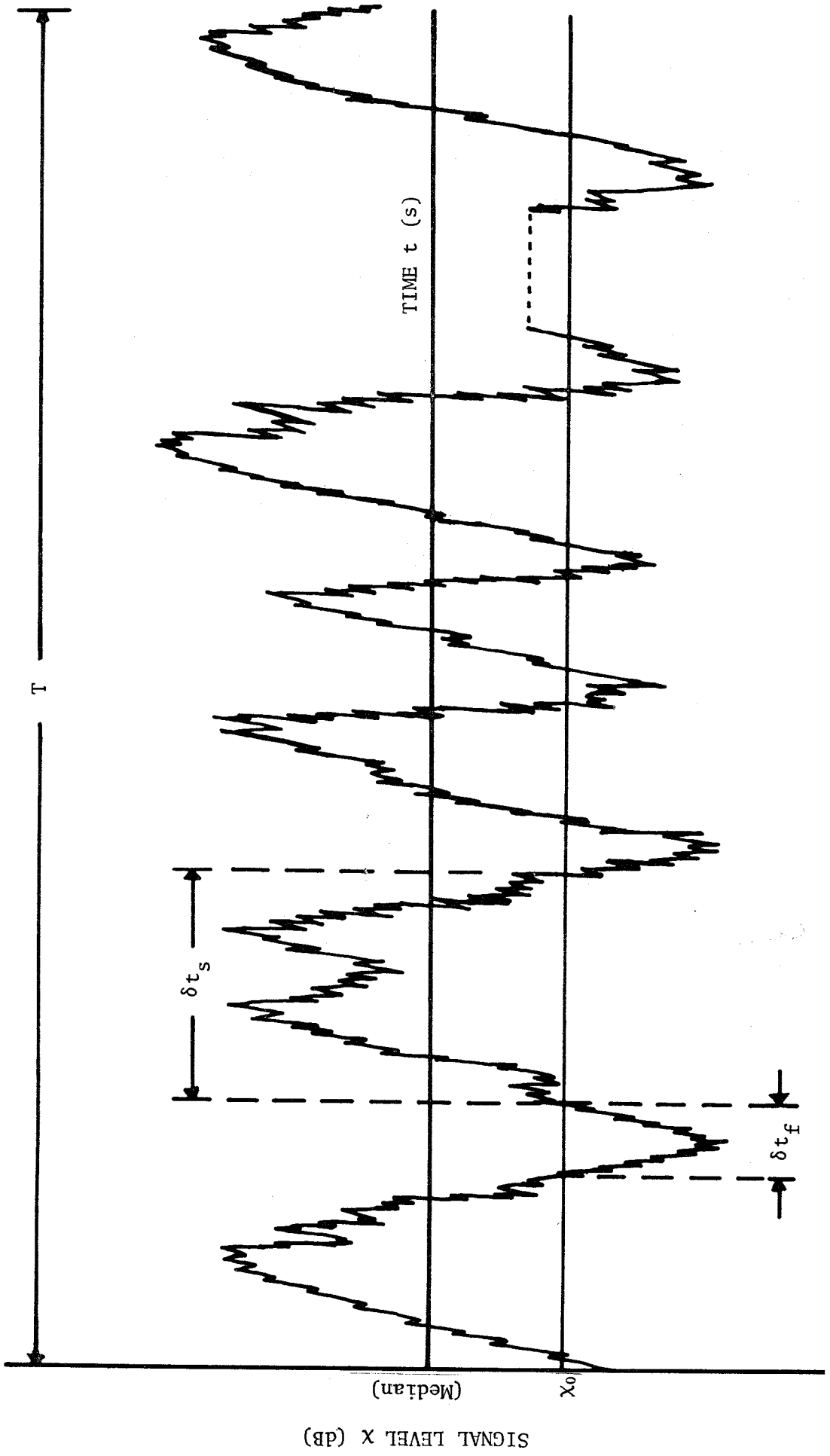

Figure 1. A schematic representation of a scintillating signal indicating the median signal level and fade margin χ_o

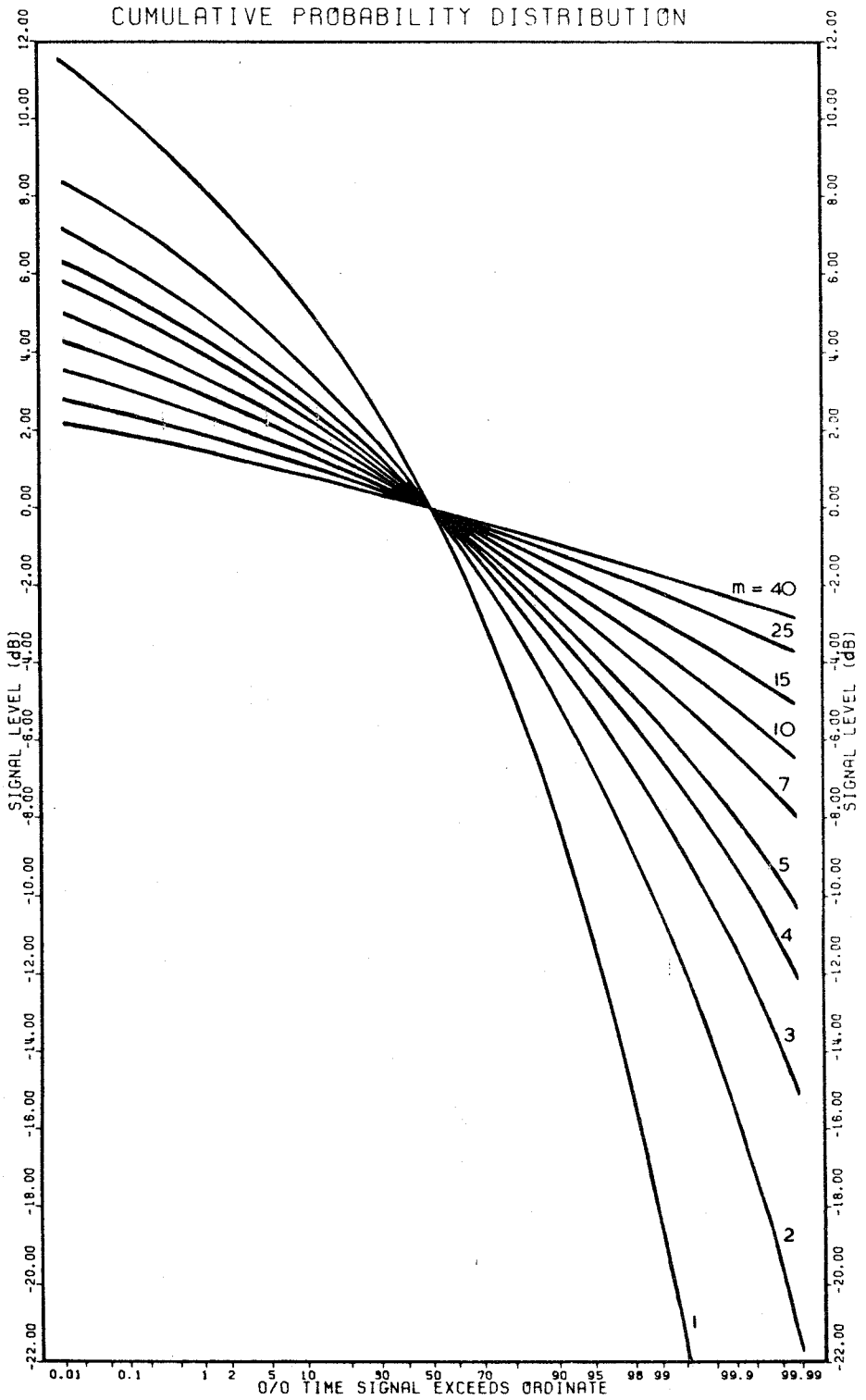

Figure 2. The cumulative form of the Nakagami m-distribution

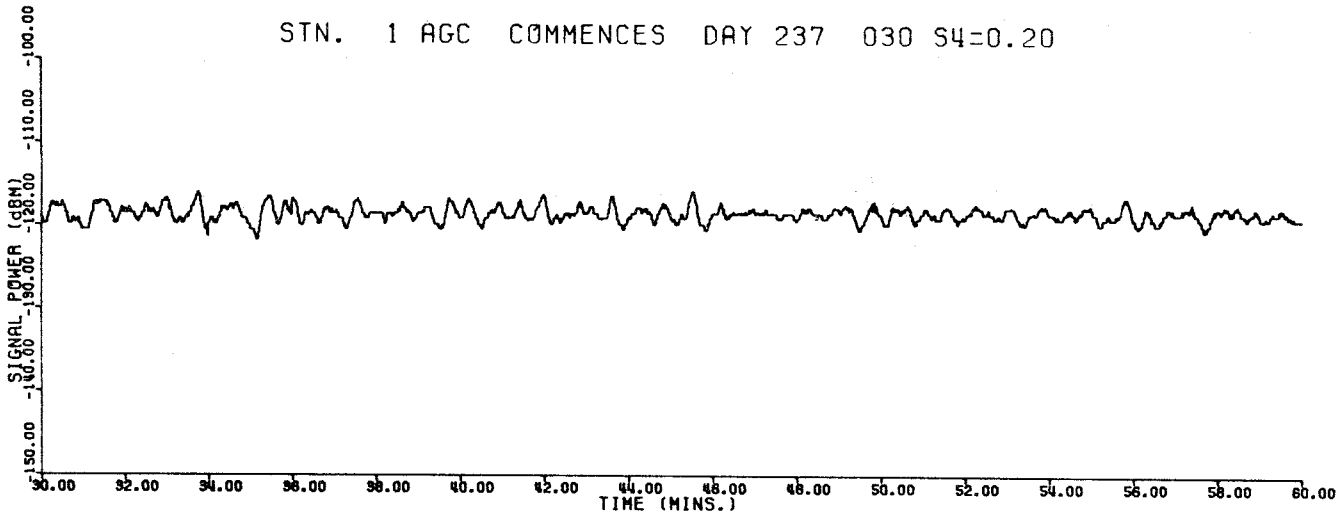

(a) analog record

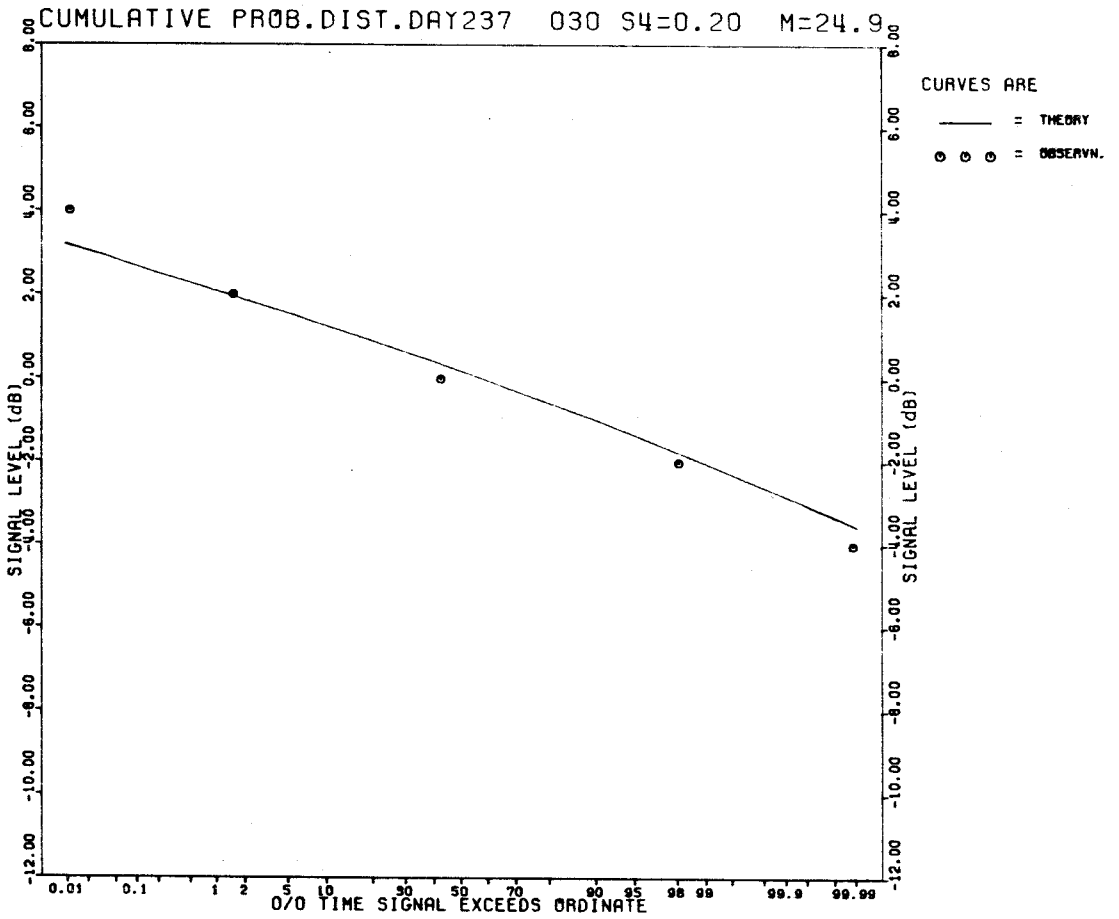

(b) cumulative amplitude probability distribution

Figure 3. Thirty minutes of scintillation (S_4 = 0.20)

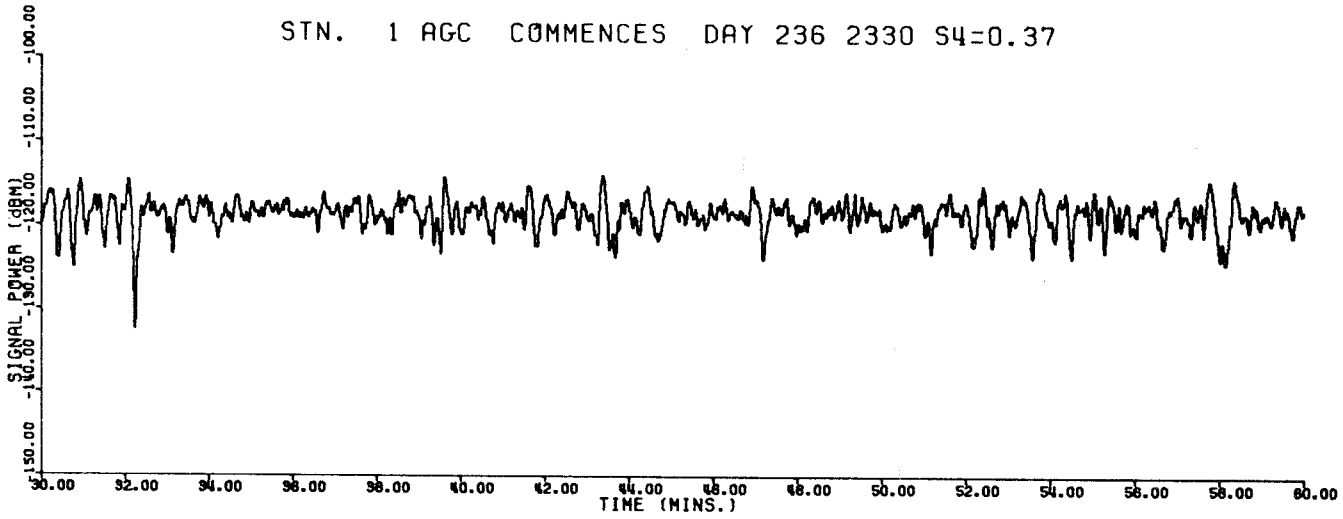

(a) analog record

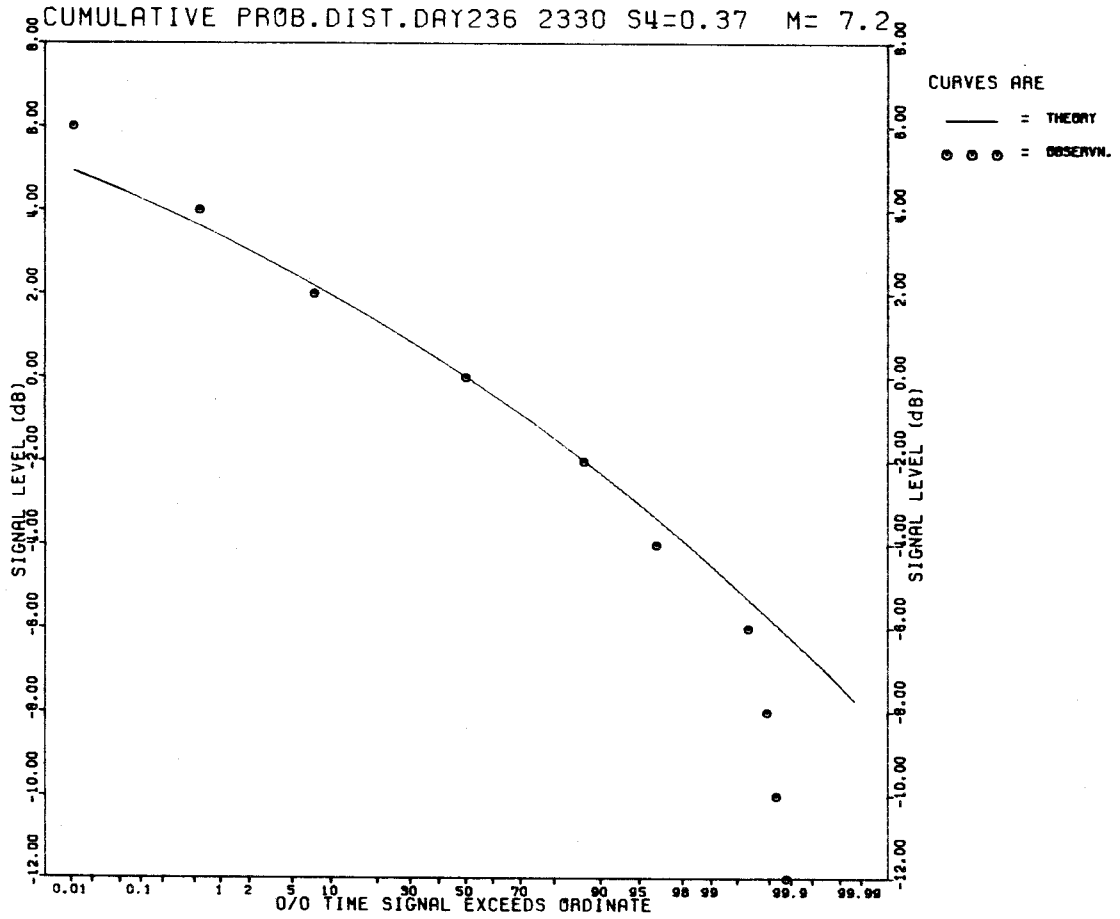

(b) cumulative amplitude probability distribution

Figure 4. Thirty minutes of scintillation (S_4 = 0.37)

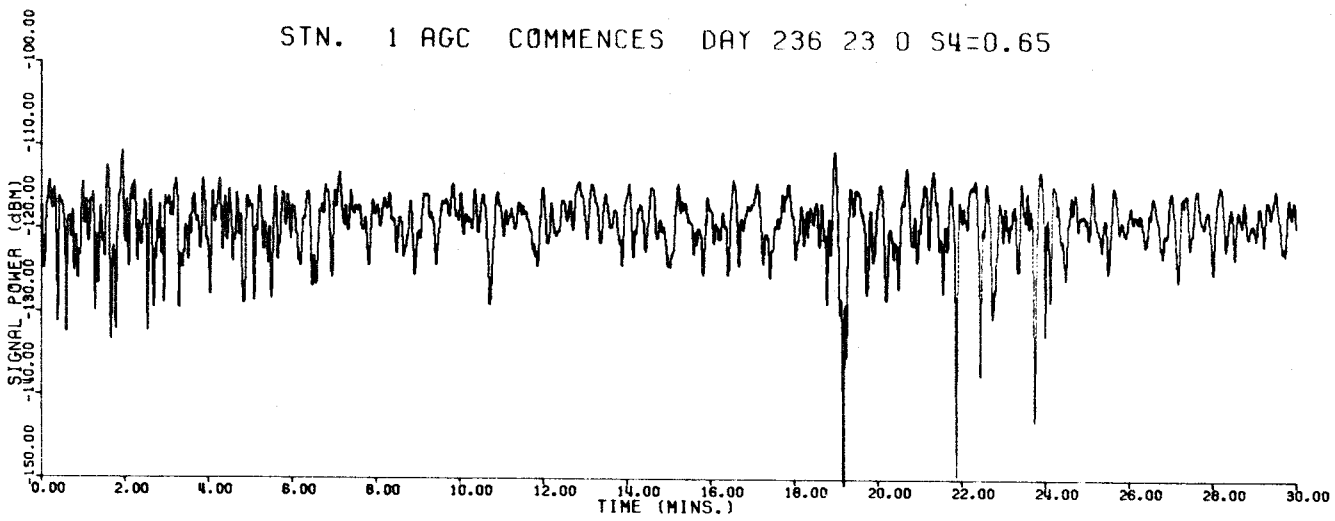

(a) analog record

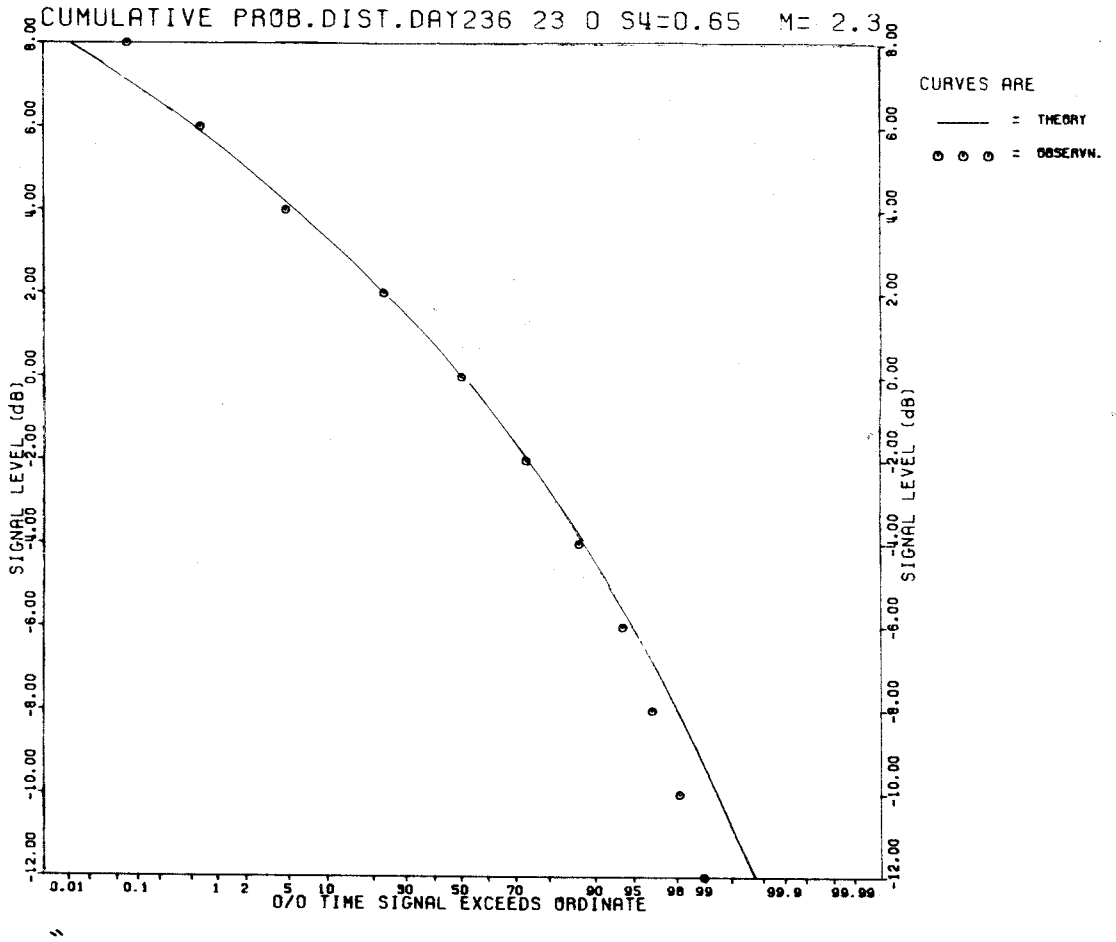

(b) cumulative amplitude probability distribution

Figure 5. Thirty minutes of scintillation (S_4 = 0.65)

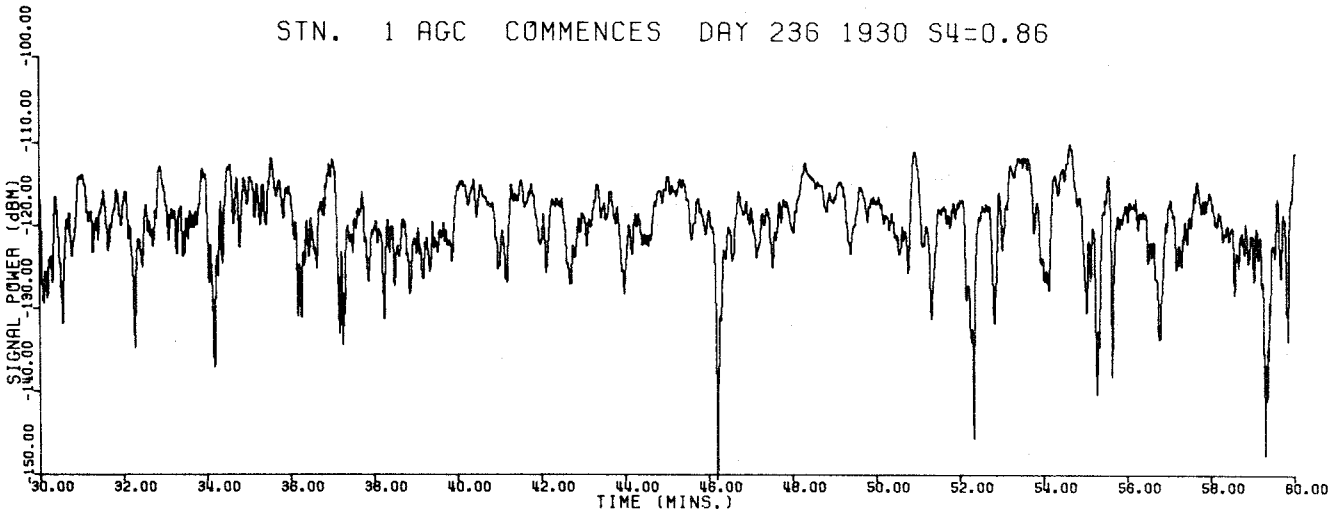

(a) analog record

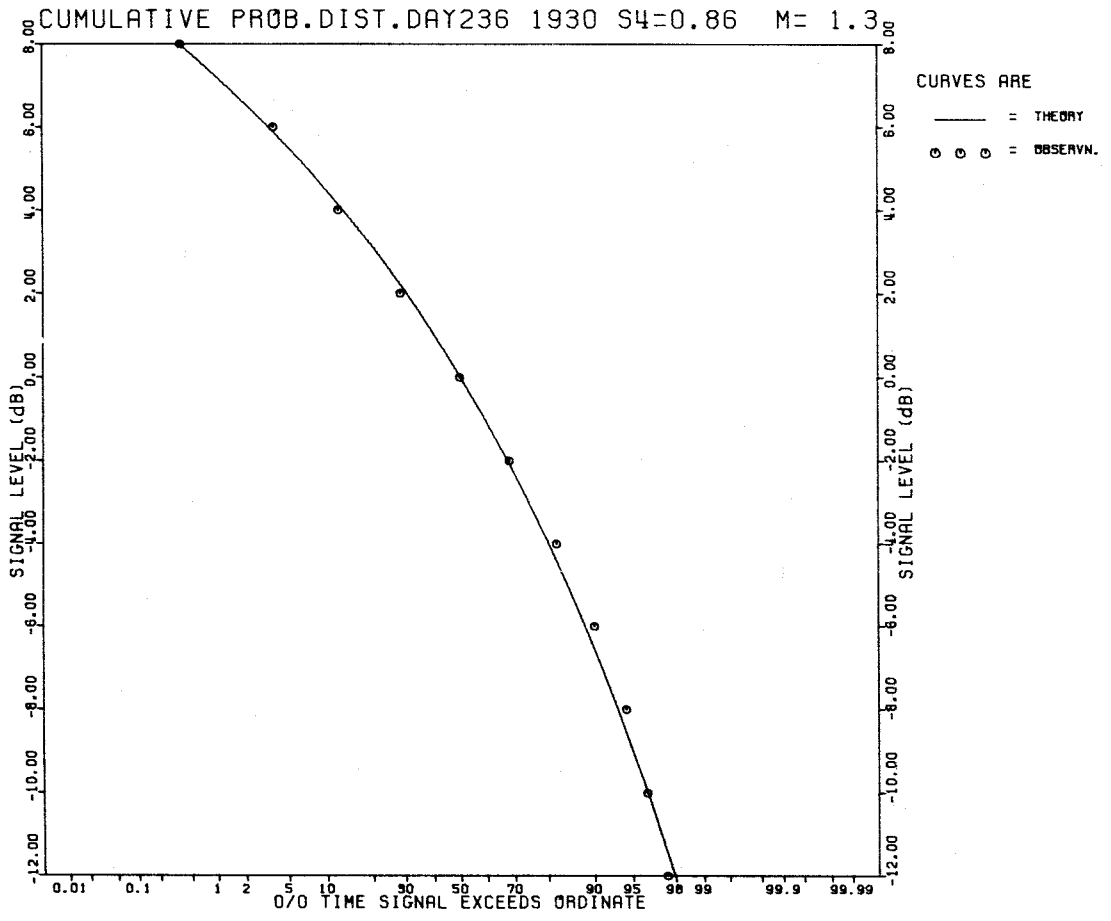

(b) cumulative amplitude probability distribution

Figure 6. Thirty minutes of scintillation (S_4 = 0.86)

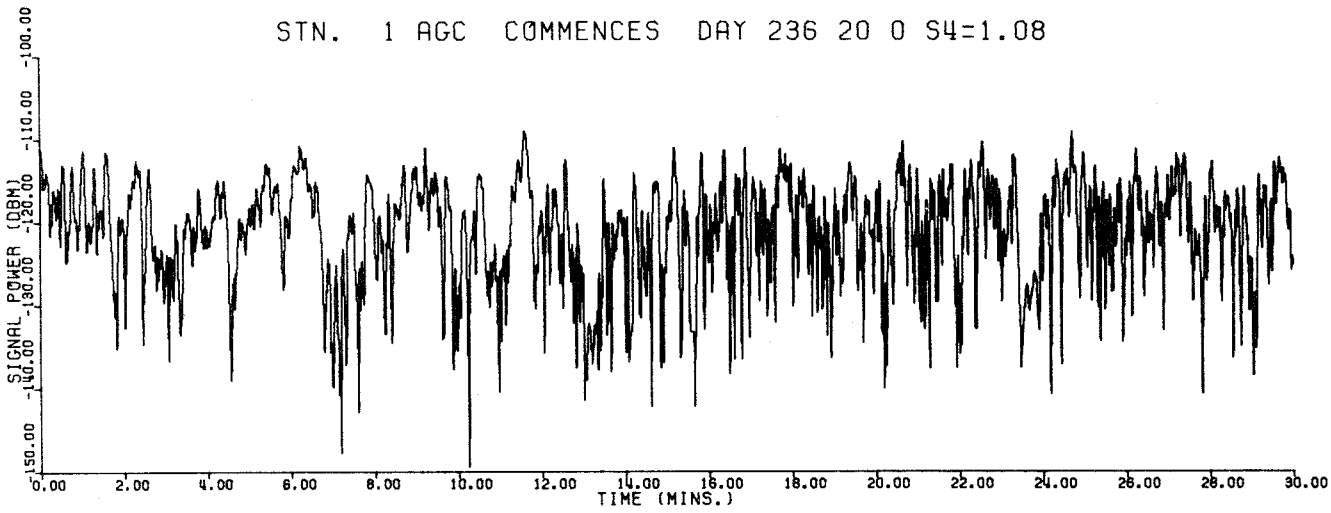

(a) analog record

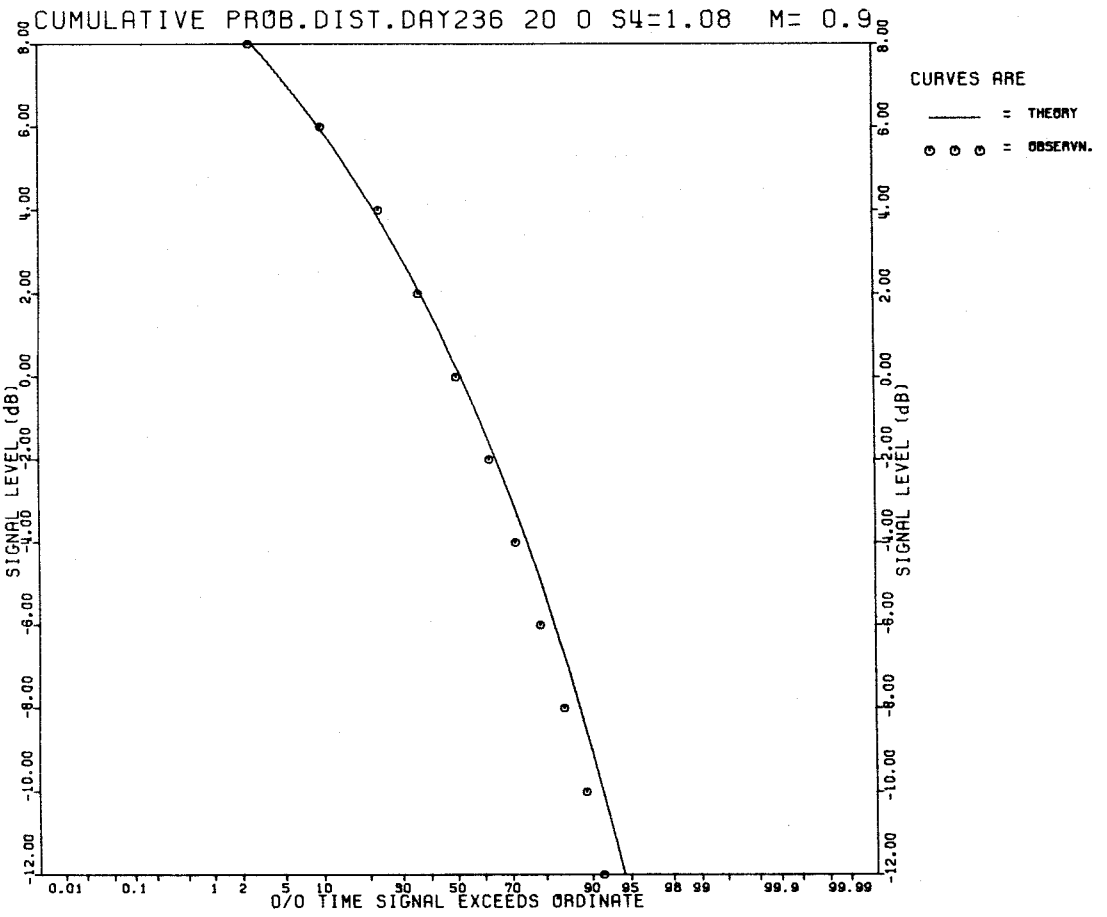

(b) cumulative amplitude probability distribution

Figure 7. Thirty minutes of scintillation (S_4 = 1.08)

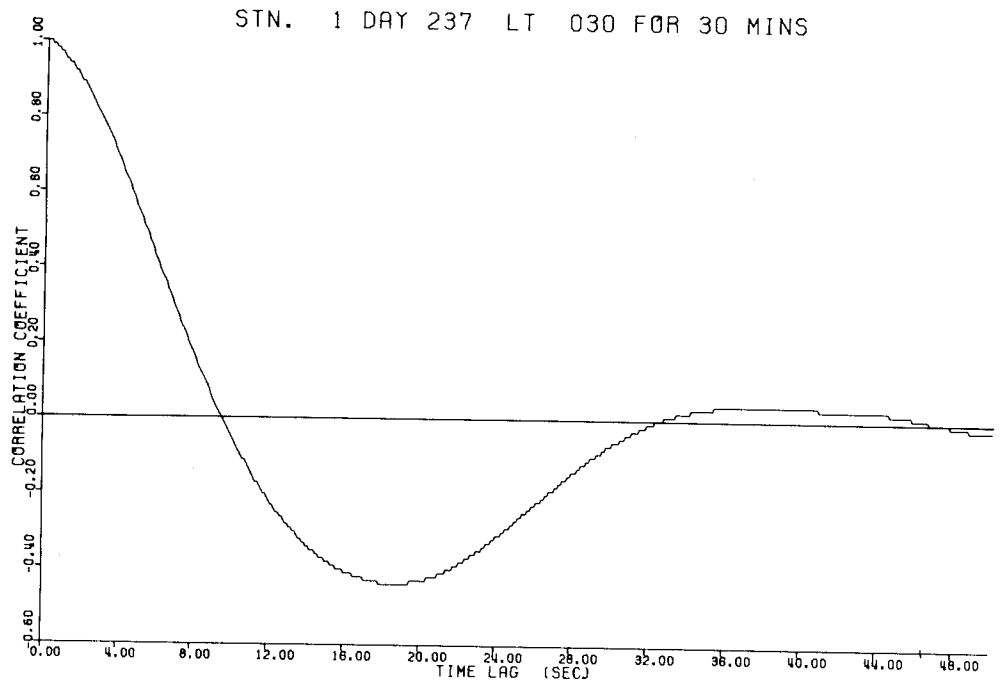

(a) autocorrelogram

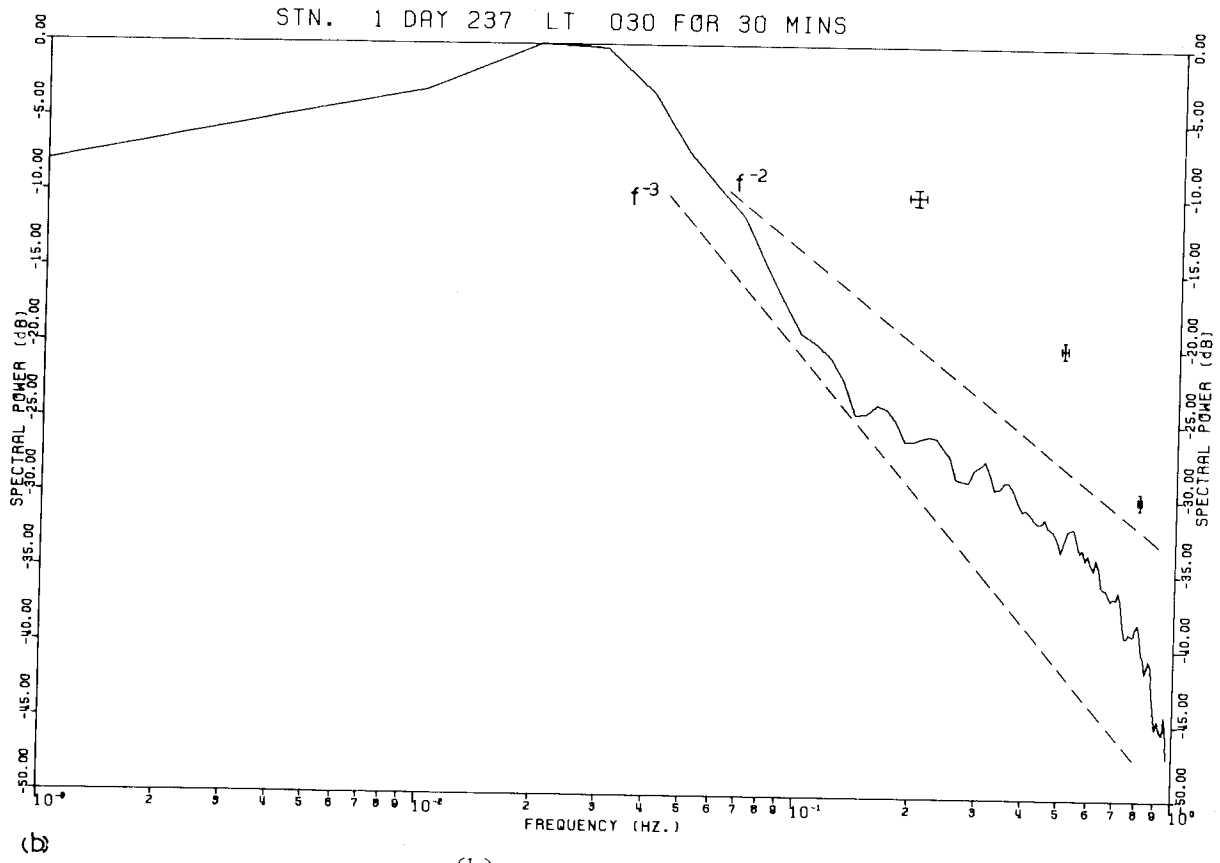

(b) power spectrum

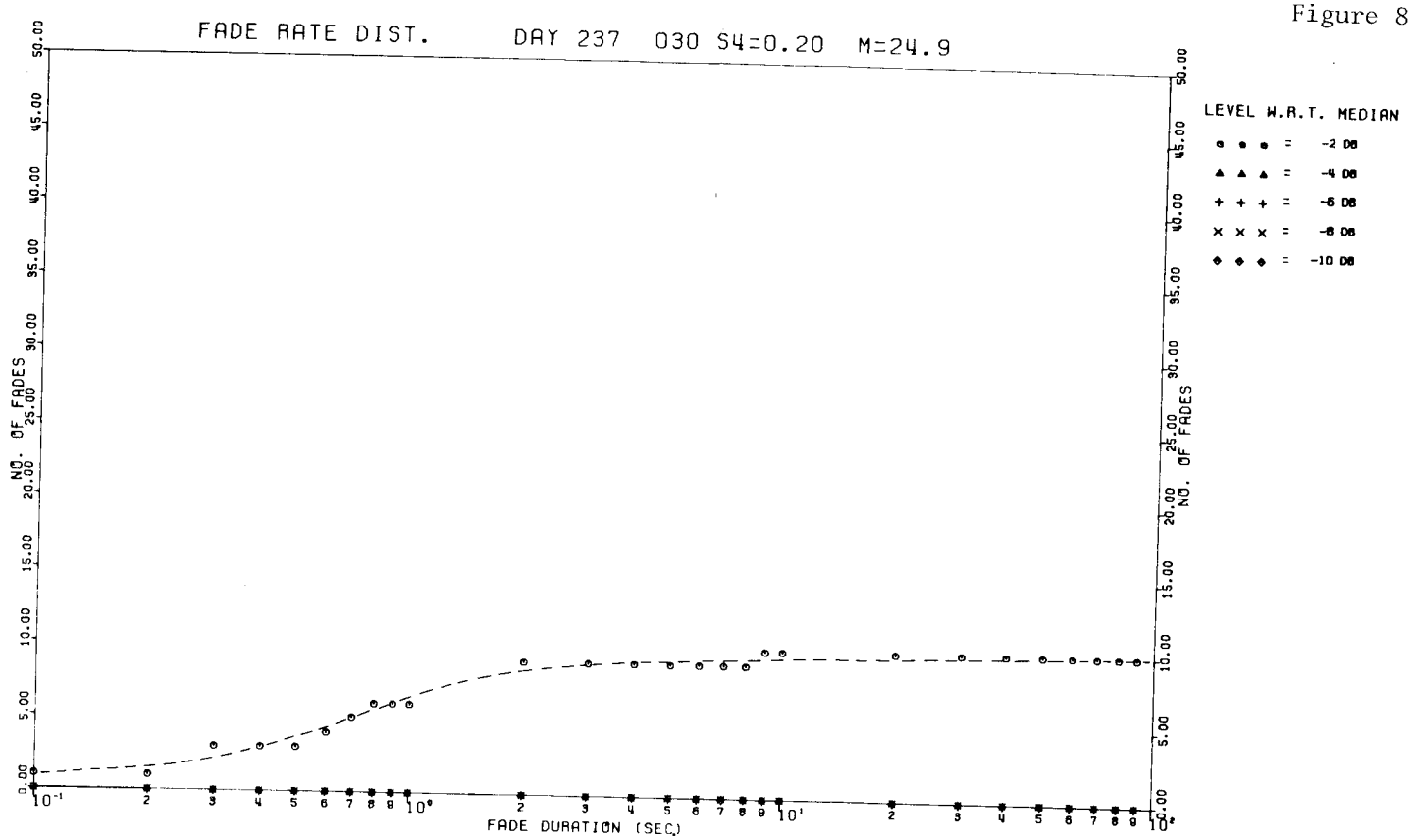

(c) cumulative fade rate distribution

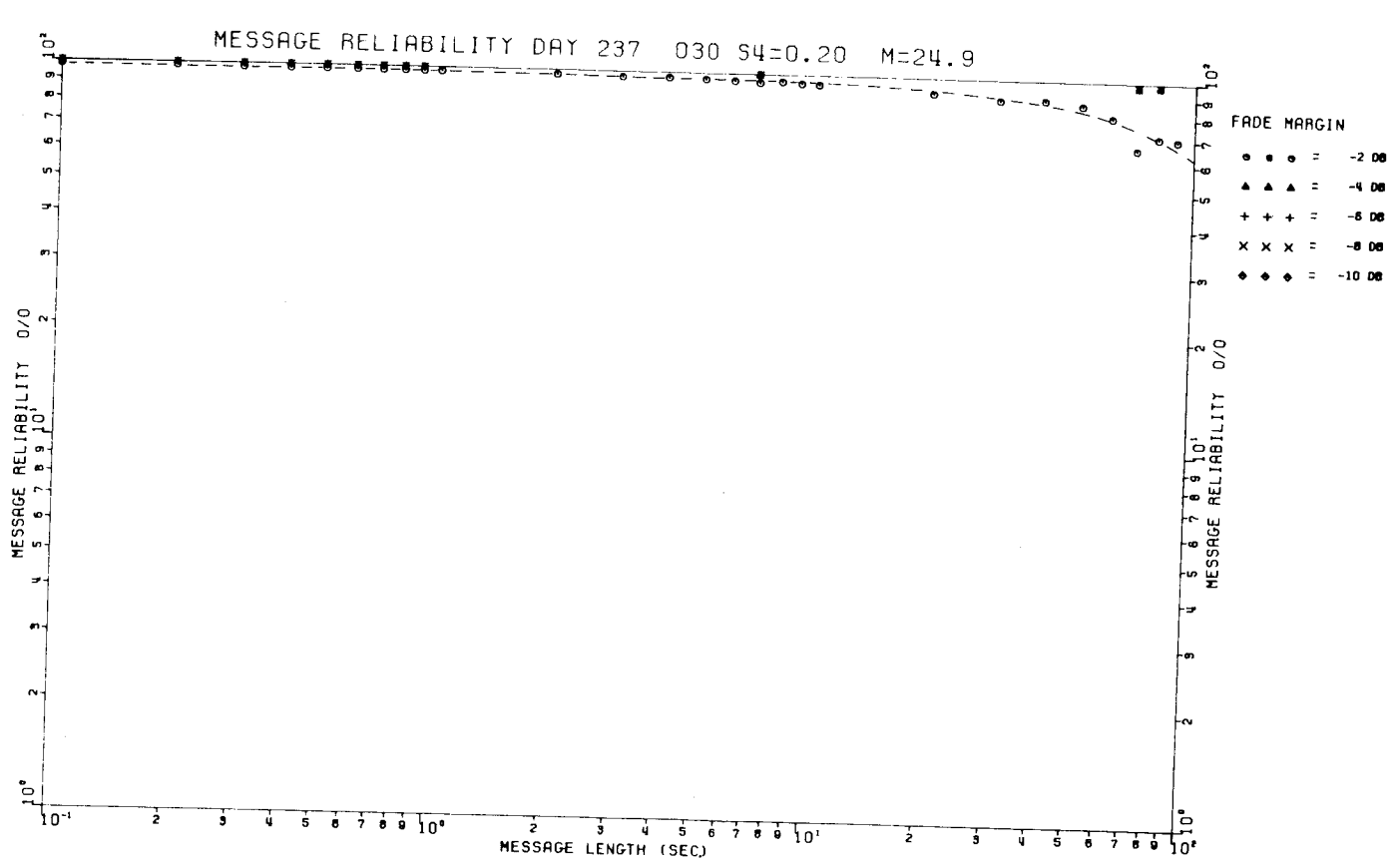

(d) message reliability distribution

Figure 8. The distributions for the scintillations shown in figure 3(a)

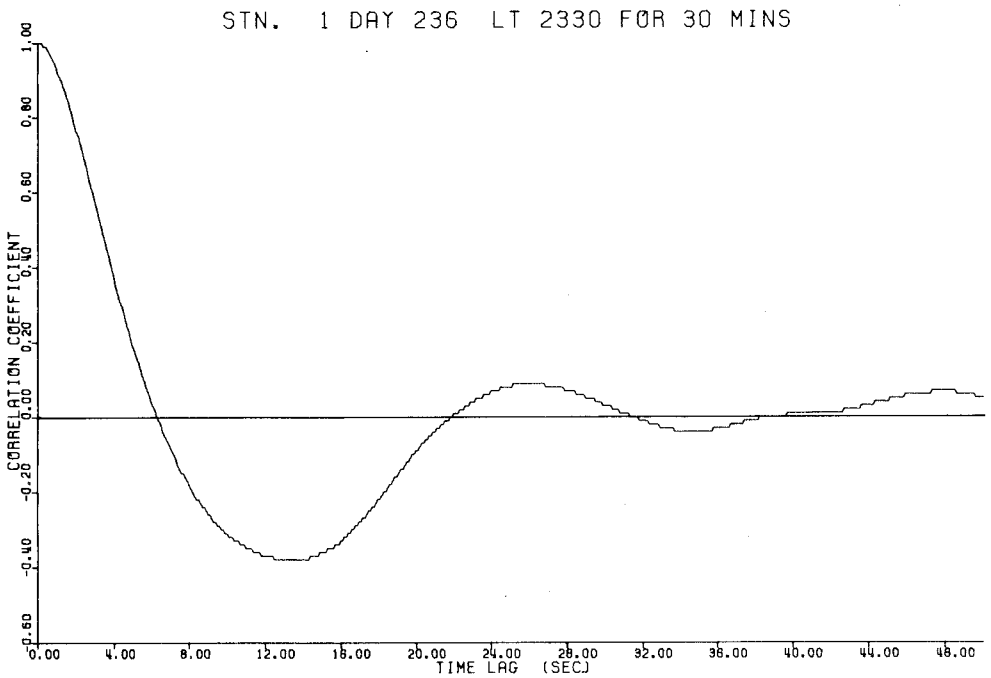

(a) autocorrelogram

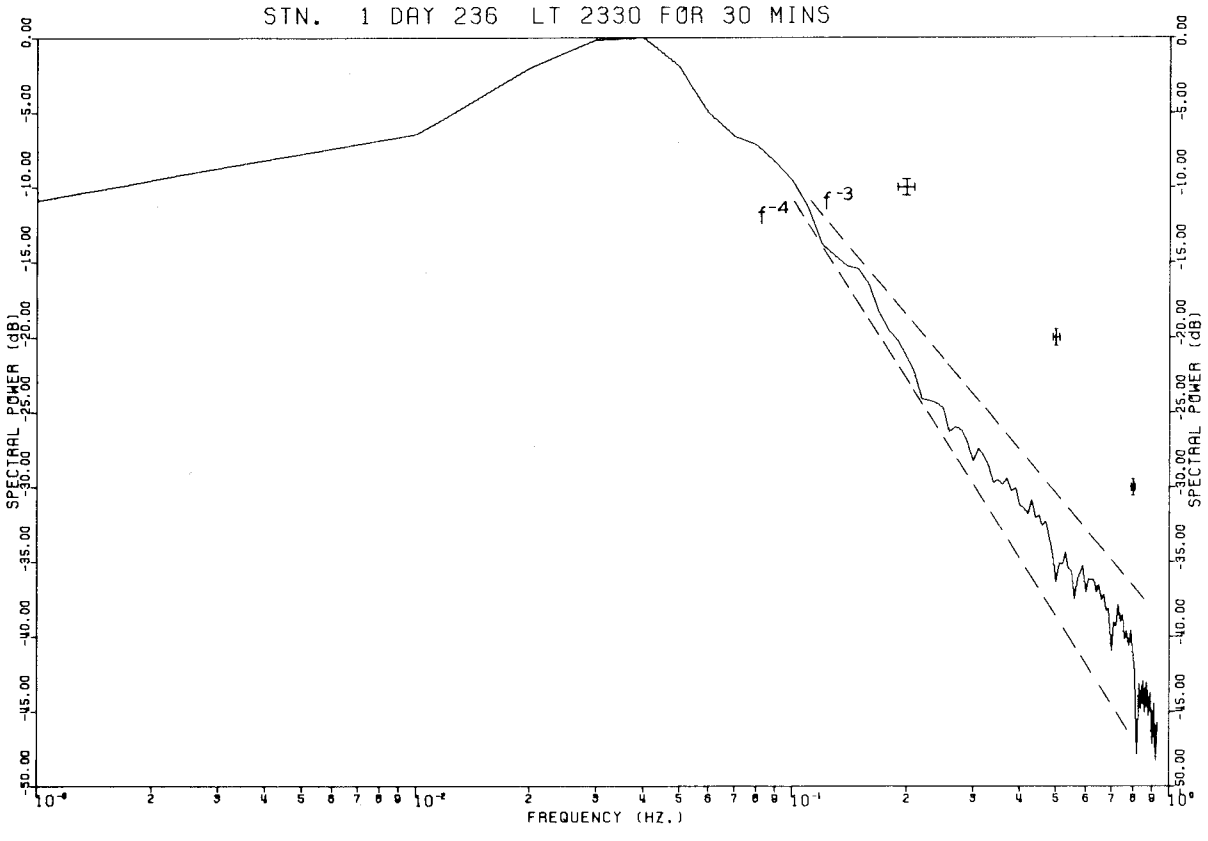

(b) power spectrum

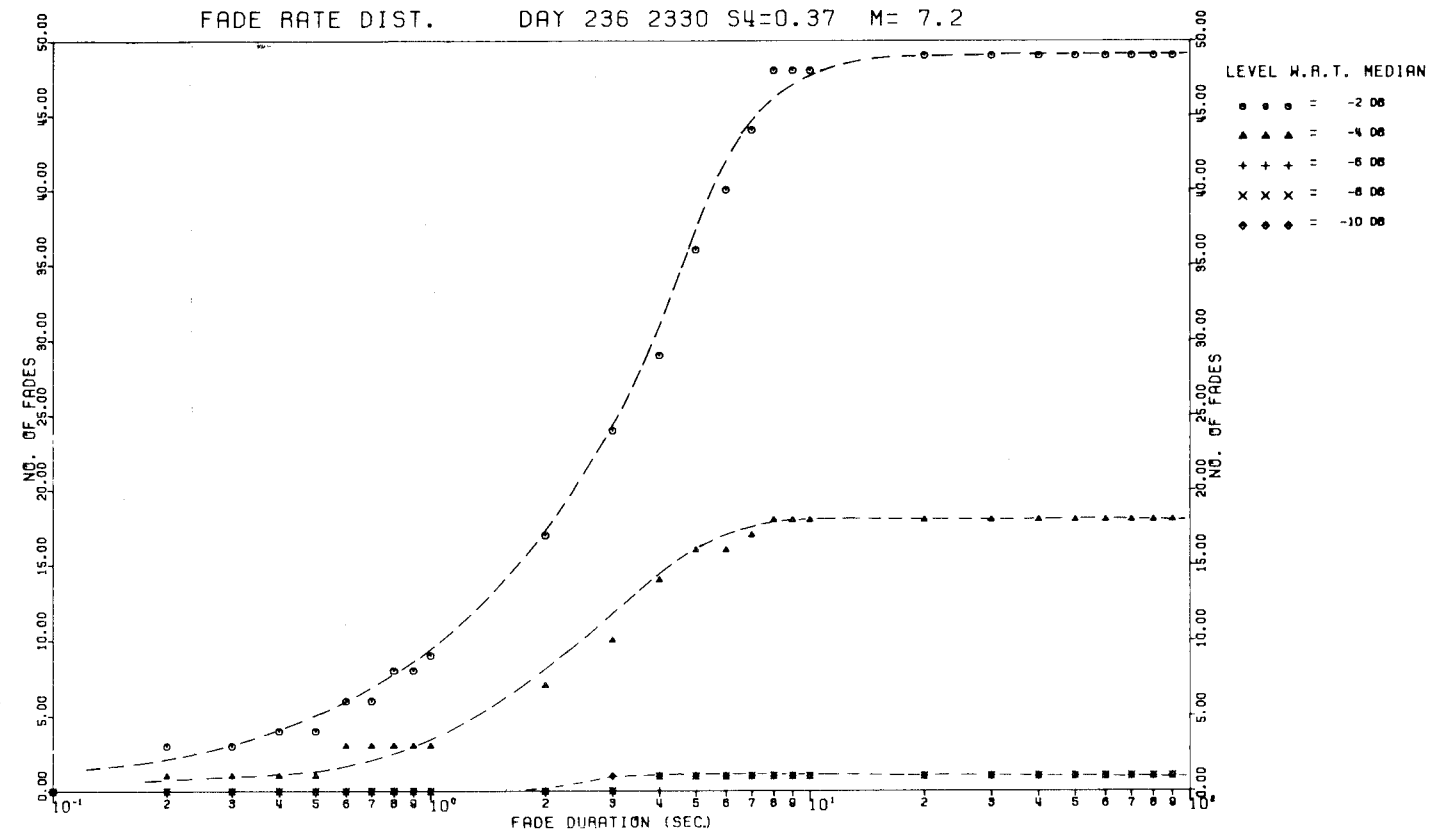

(c) cumulative fade rate distribution

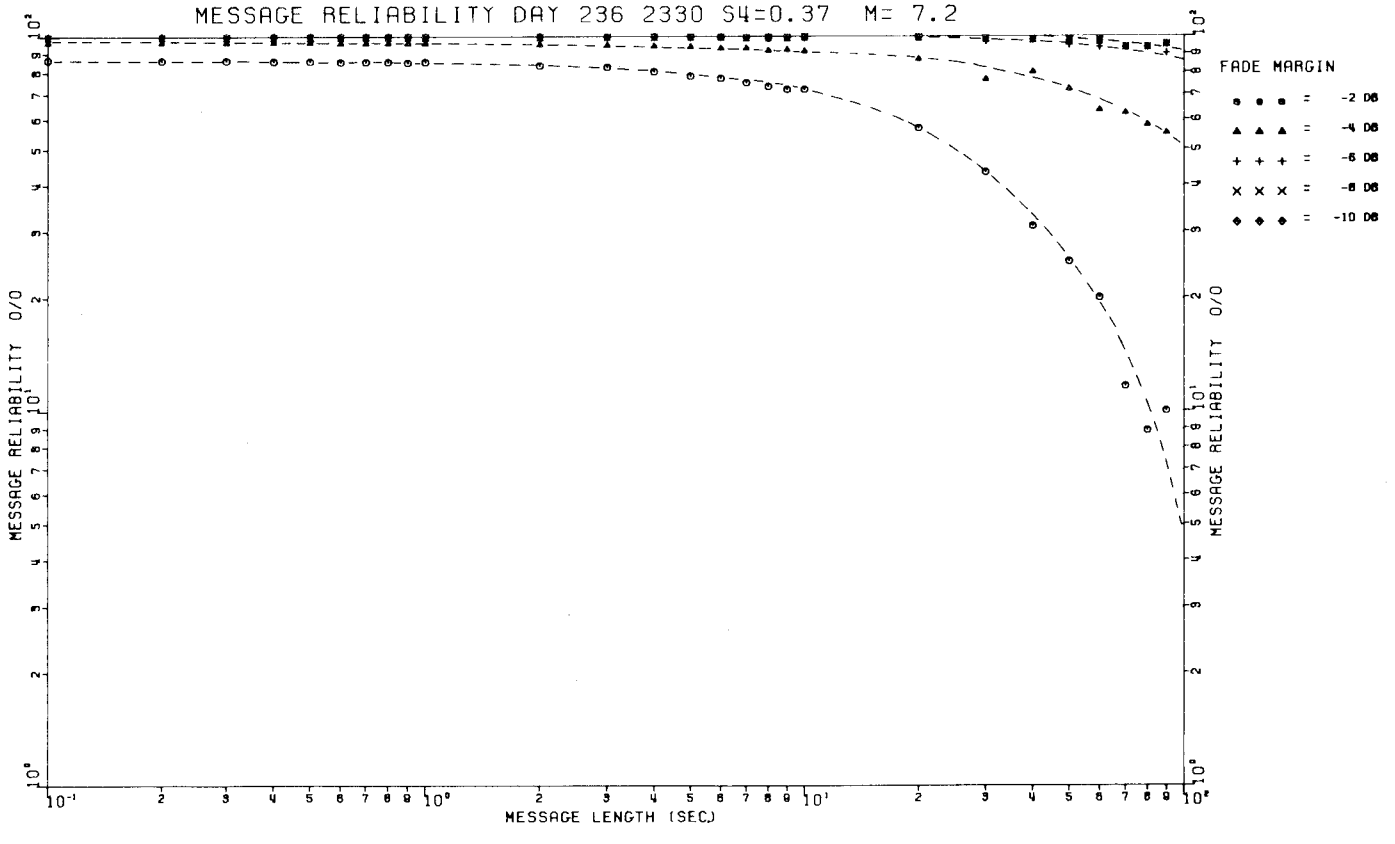

(d) message reliability distribution

Figure 9. The distributions for the scintillations shown in figure 4(a)

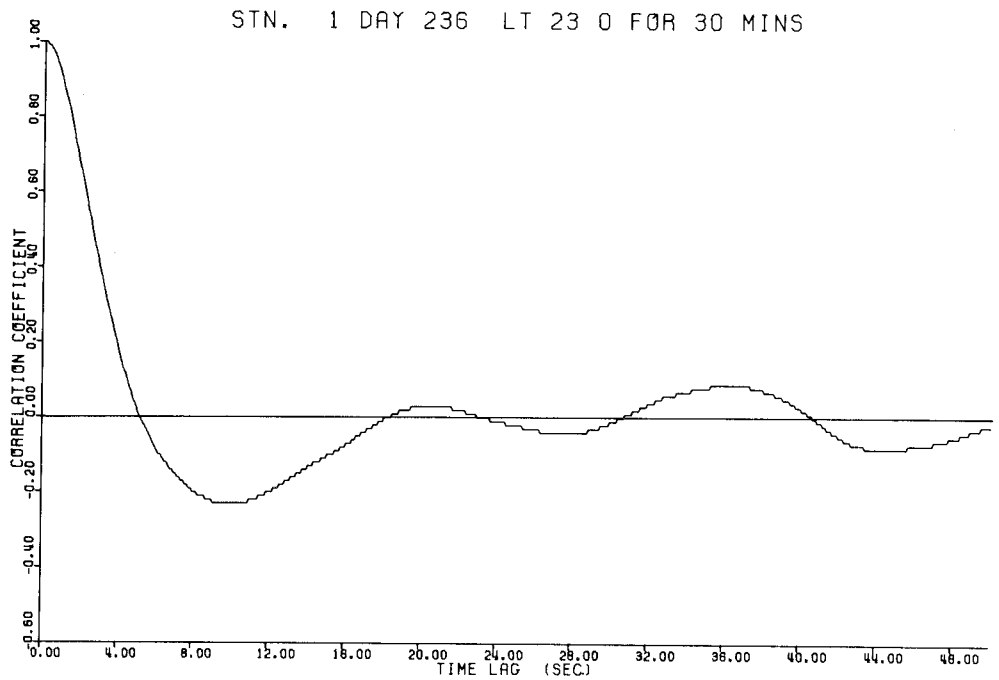

(a) autocorrelogram

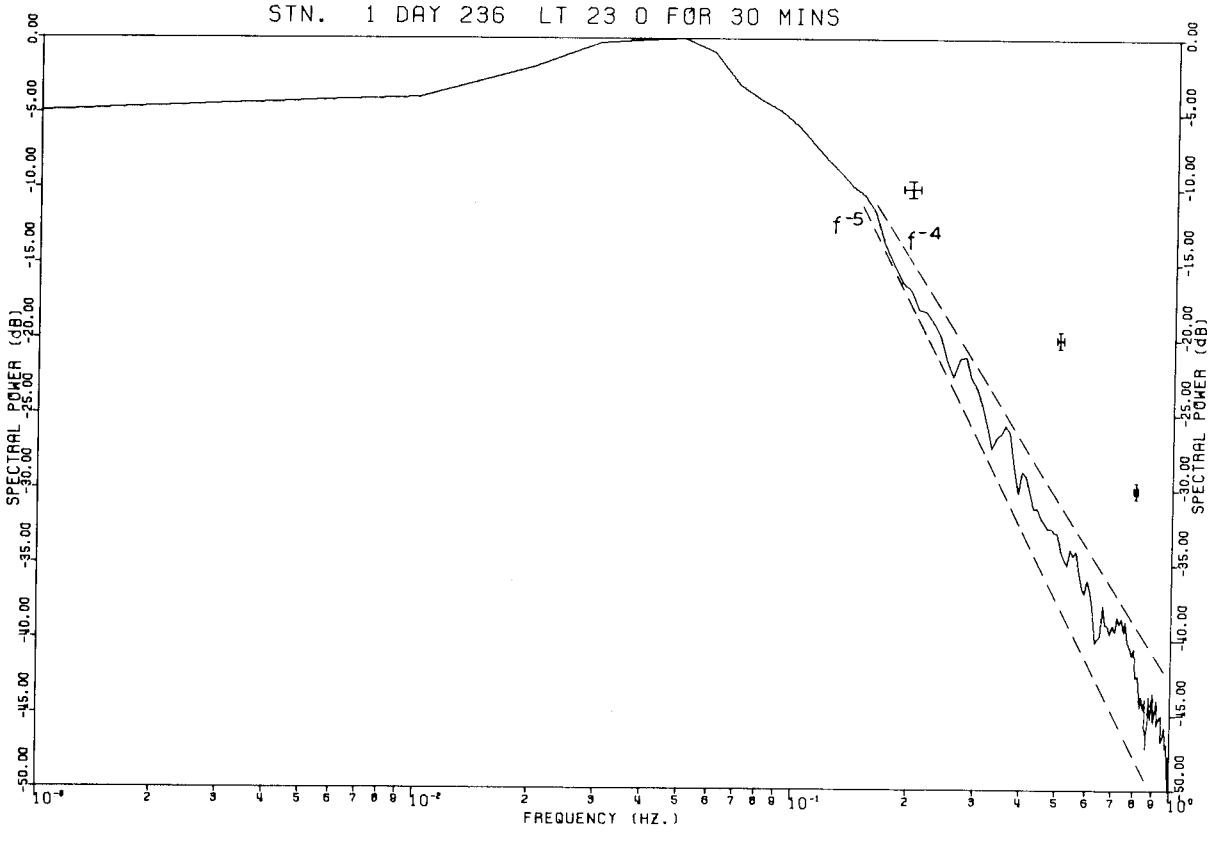

(b) power spectrum

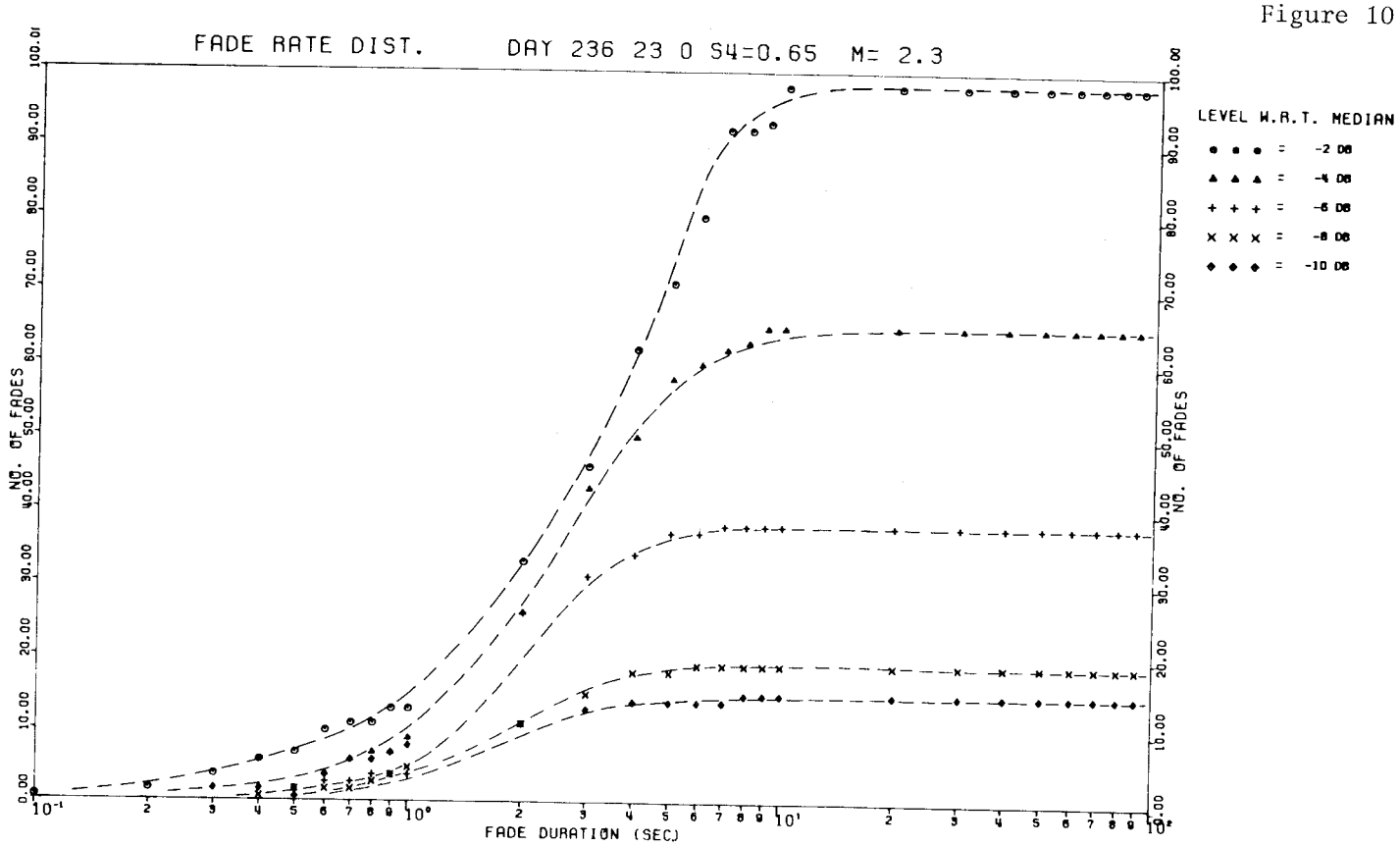

(c) cumulative fade rate distribution

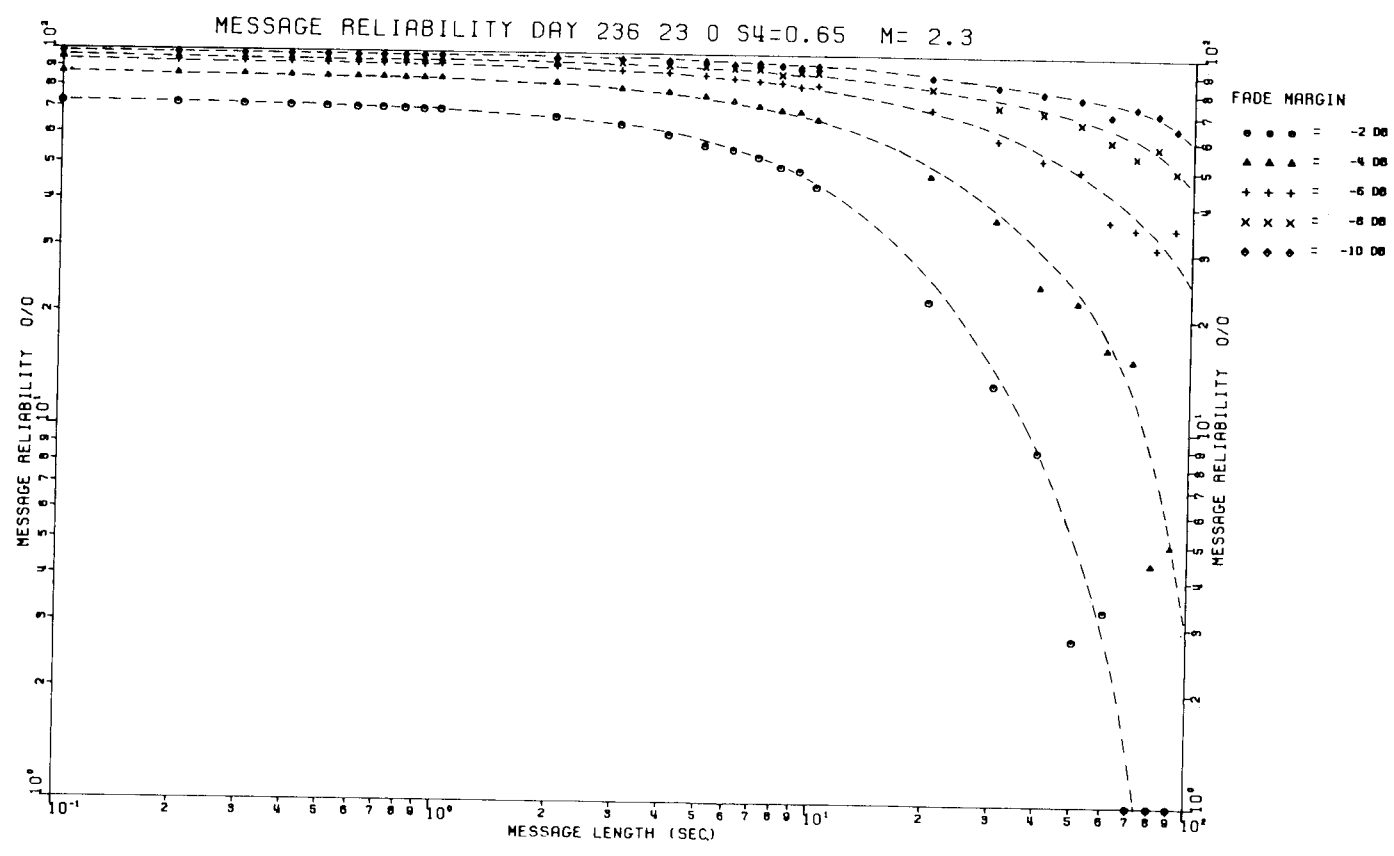

(d) message reliability distribution

Figure 10. The distributions for the scintillations shown in figure 5(a)

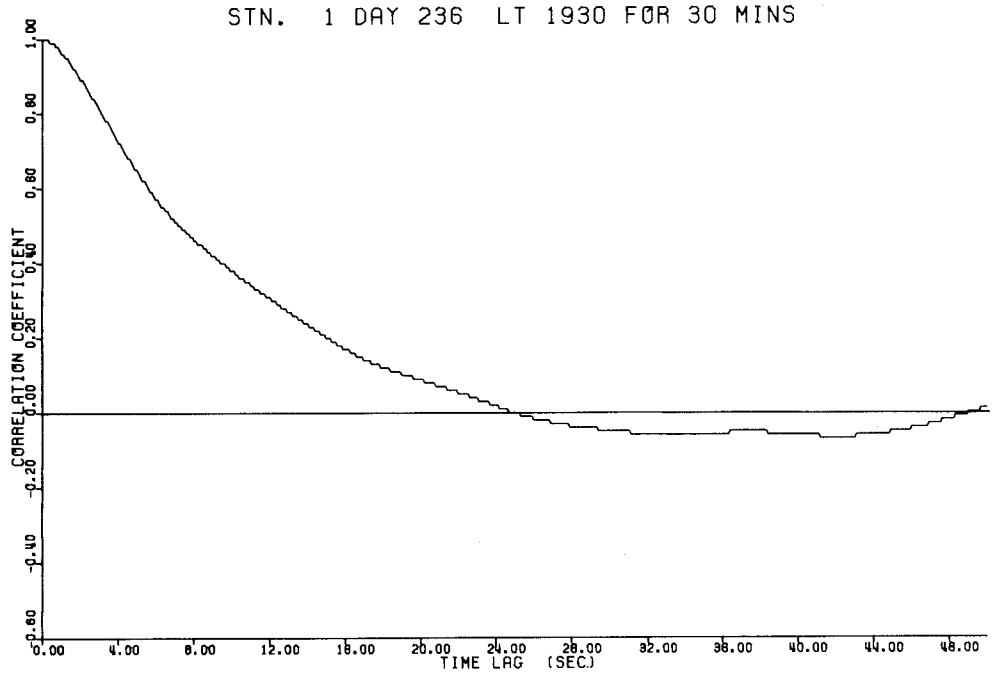

(a) autocorrelogram

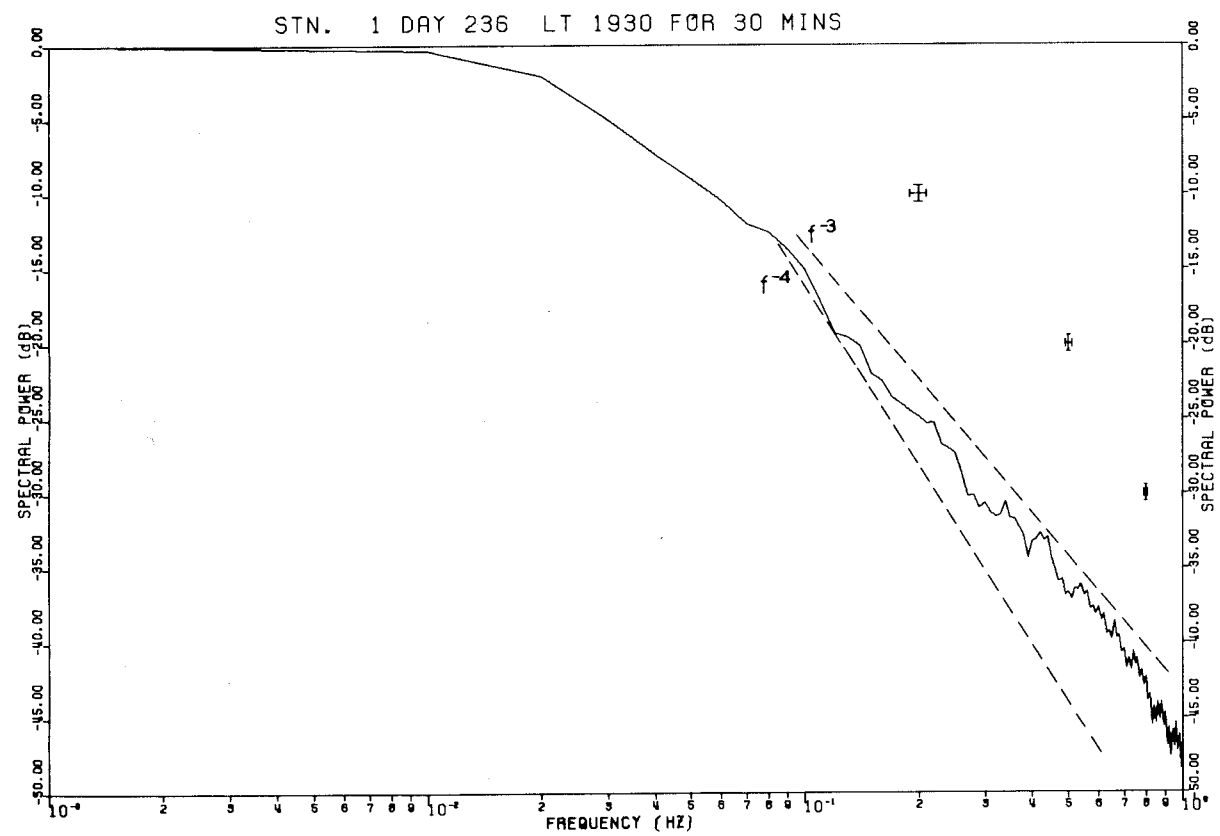

(b) power spectrum

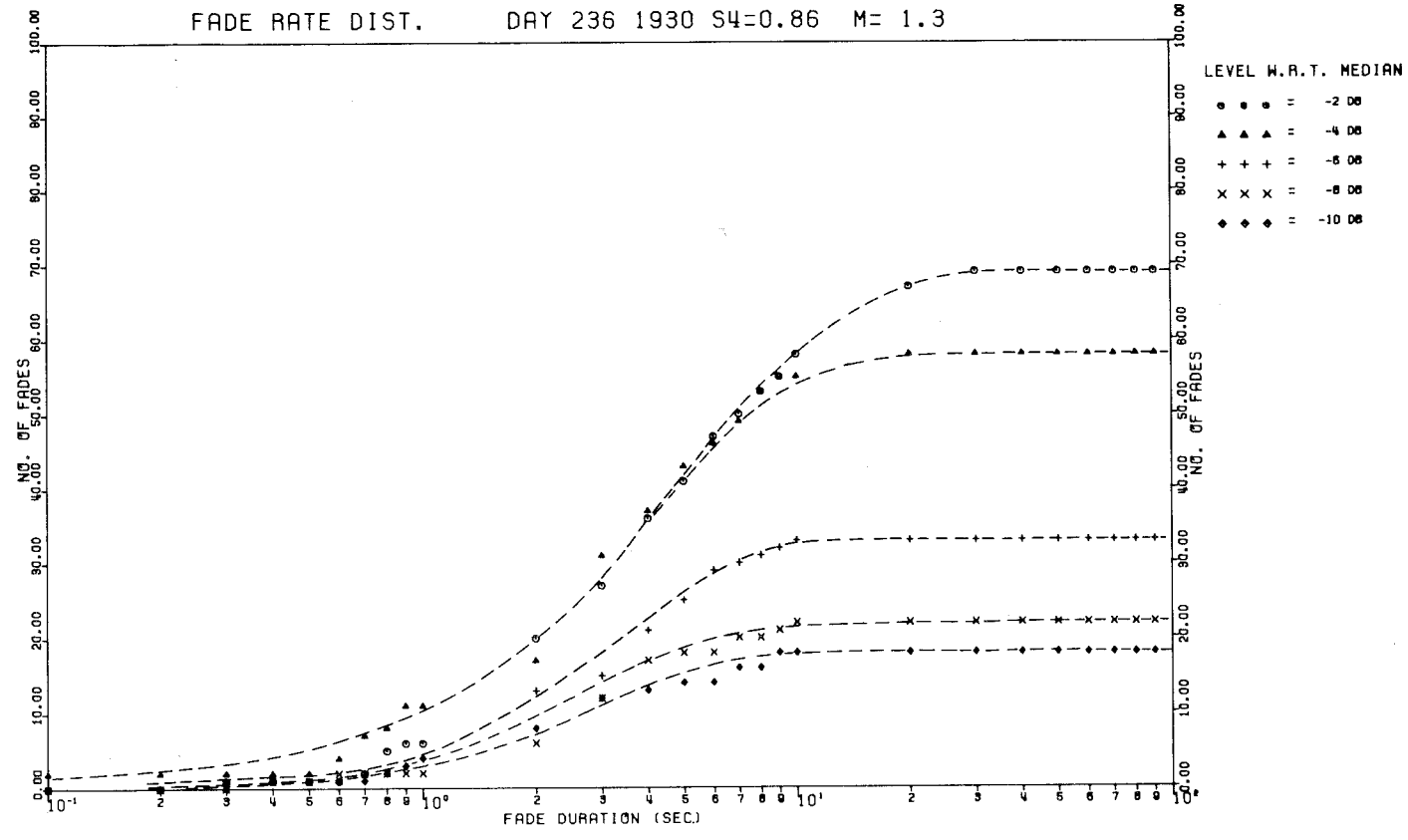

(c) cumulative fade rate distribution

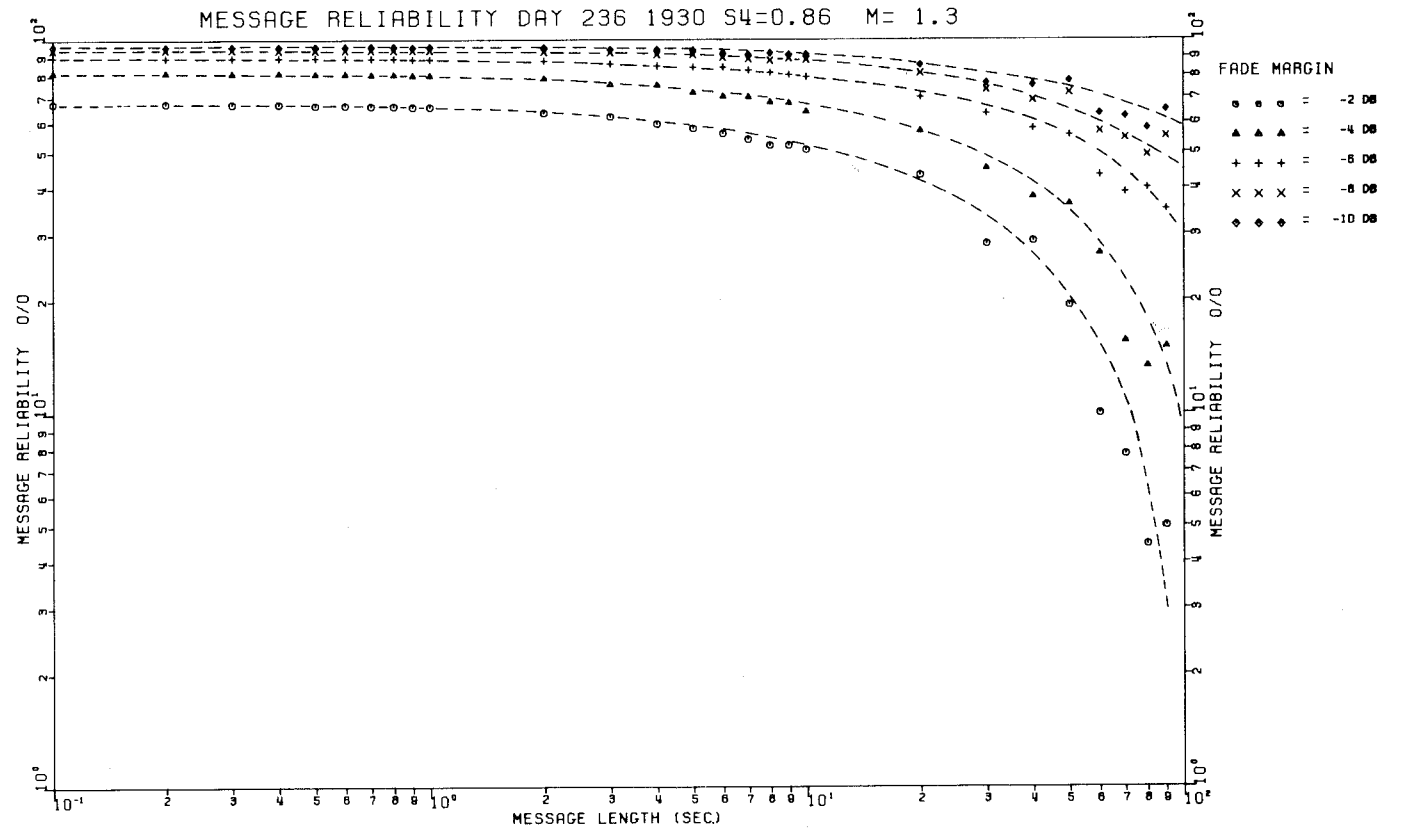

(d) message reliability distribution

Figure 11. The distributions for the scintillations shown in figure 6(a)

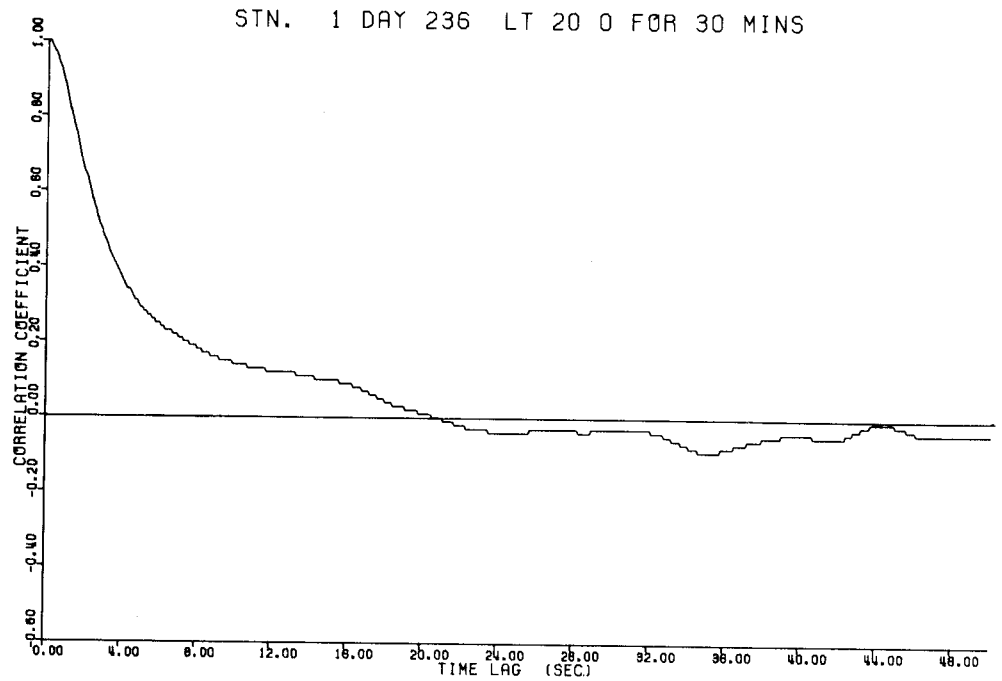

(a) autocorrelogram

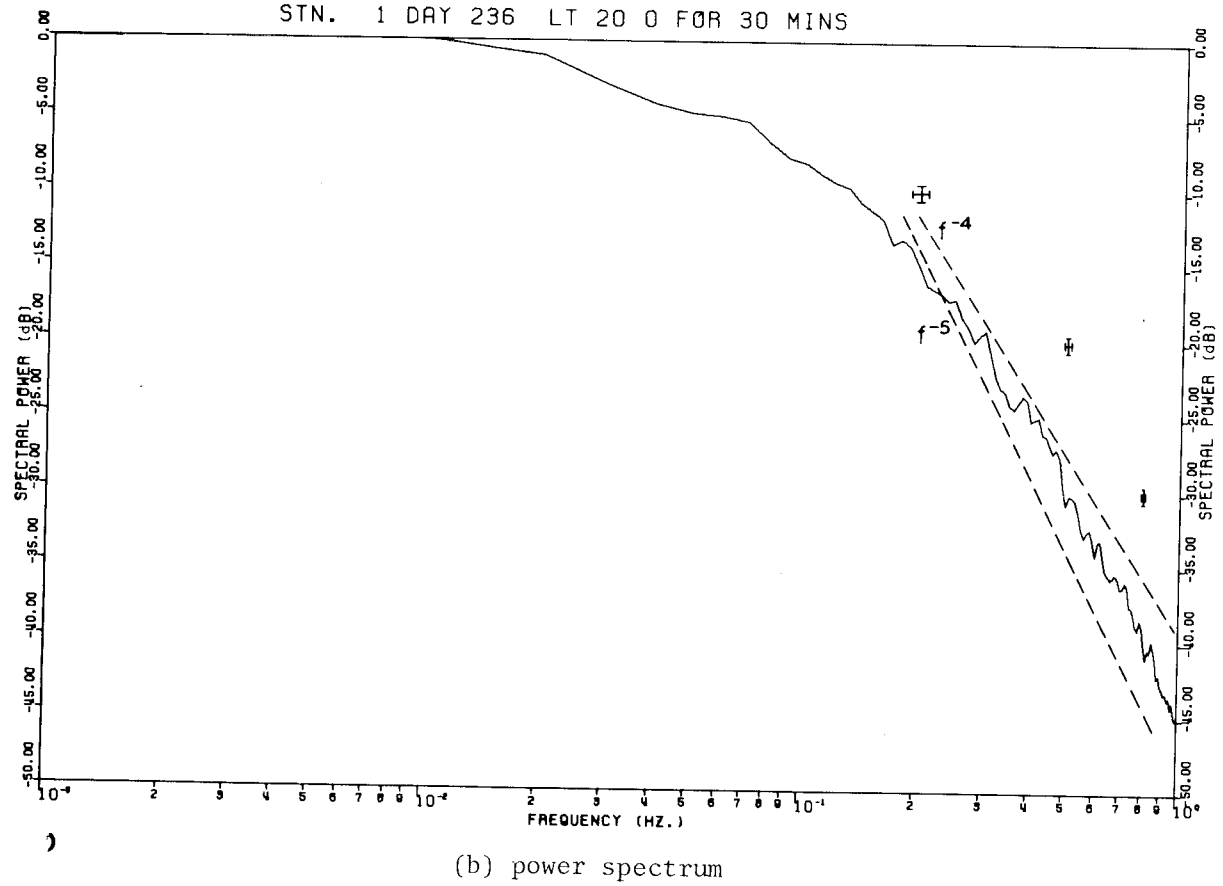

(b) power spectrum

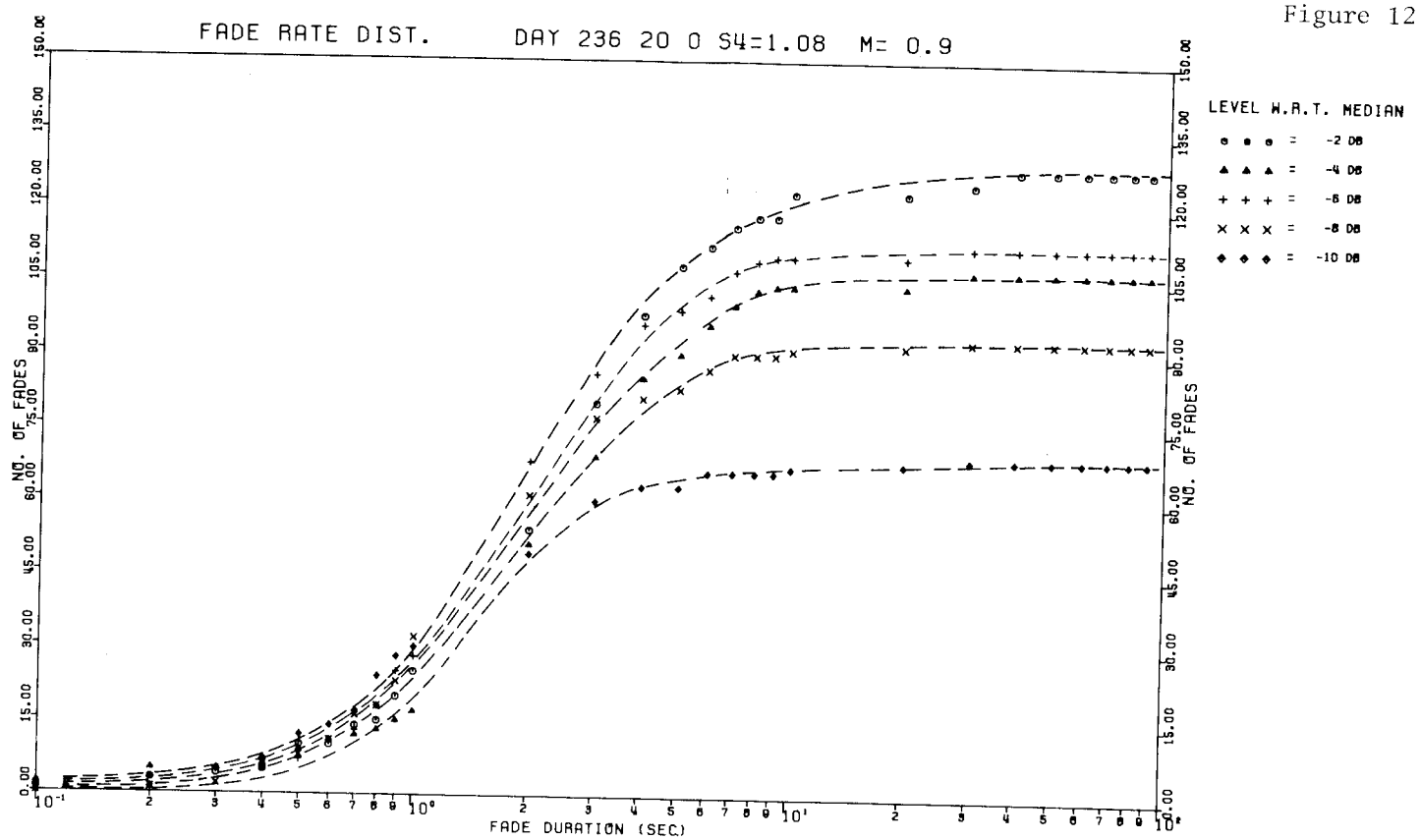

(c) cumulative fade rate distribution

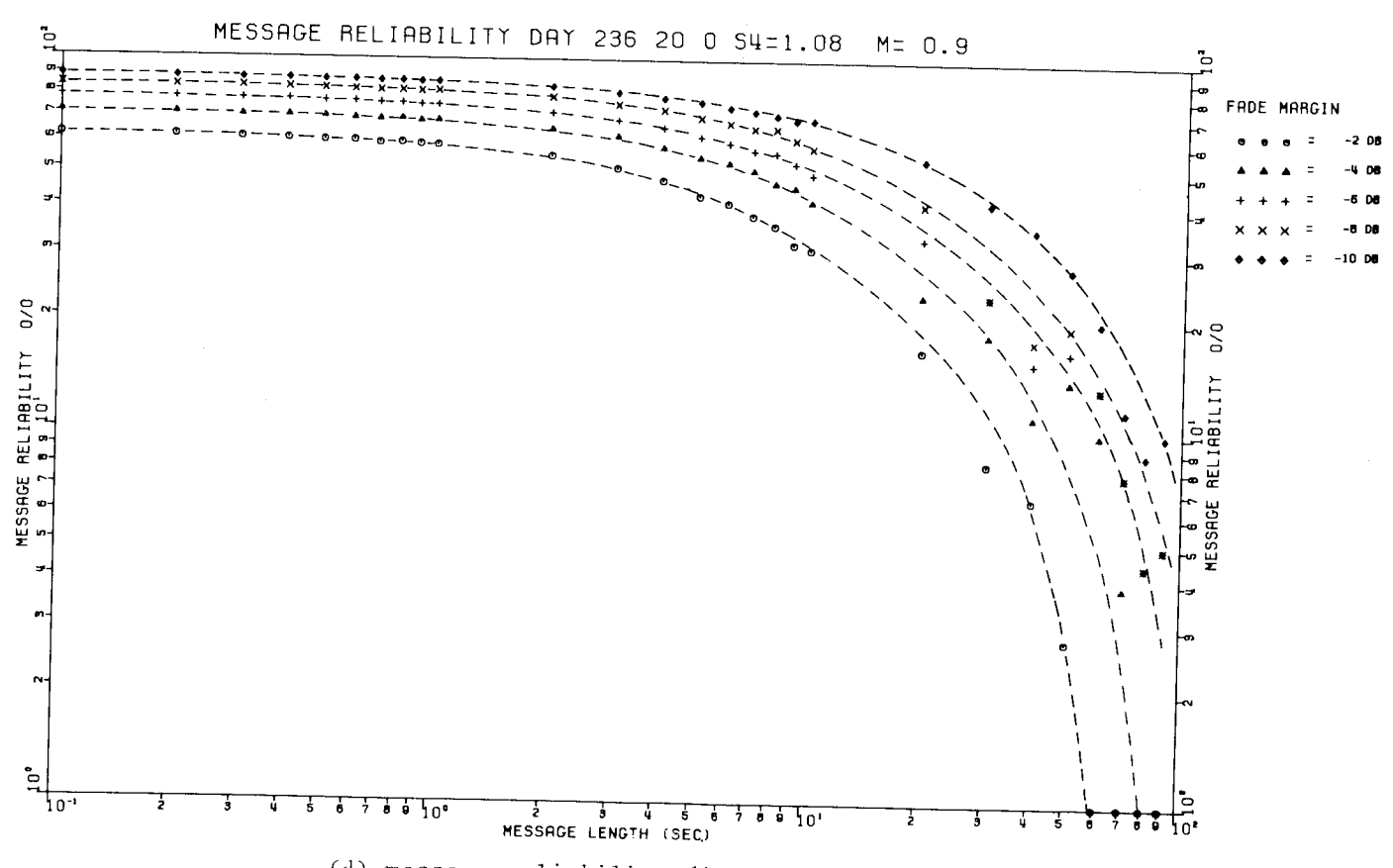

(d) message reliability distribution

Figure 12. The distributions for the scintillations shown in figure 7(a)

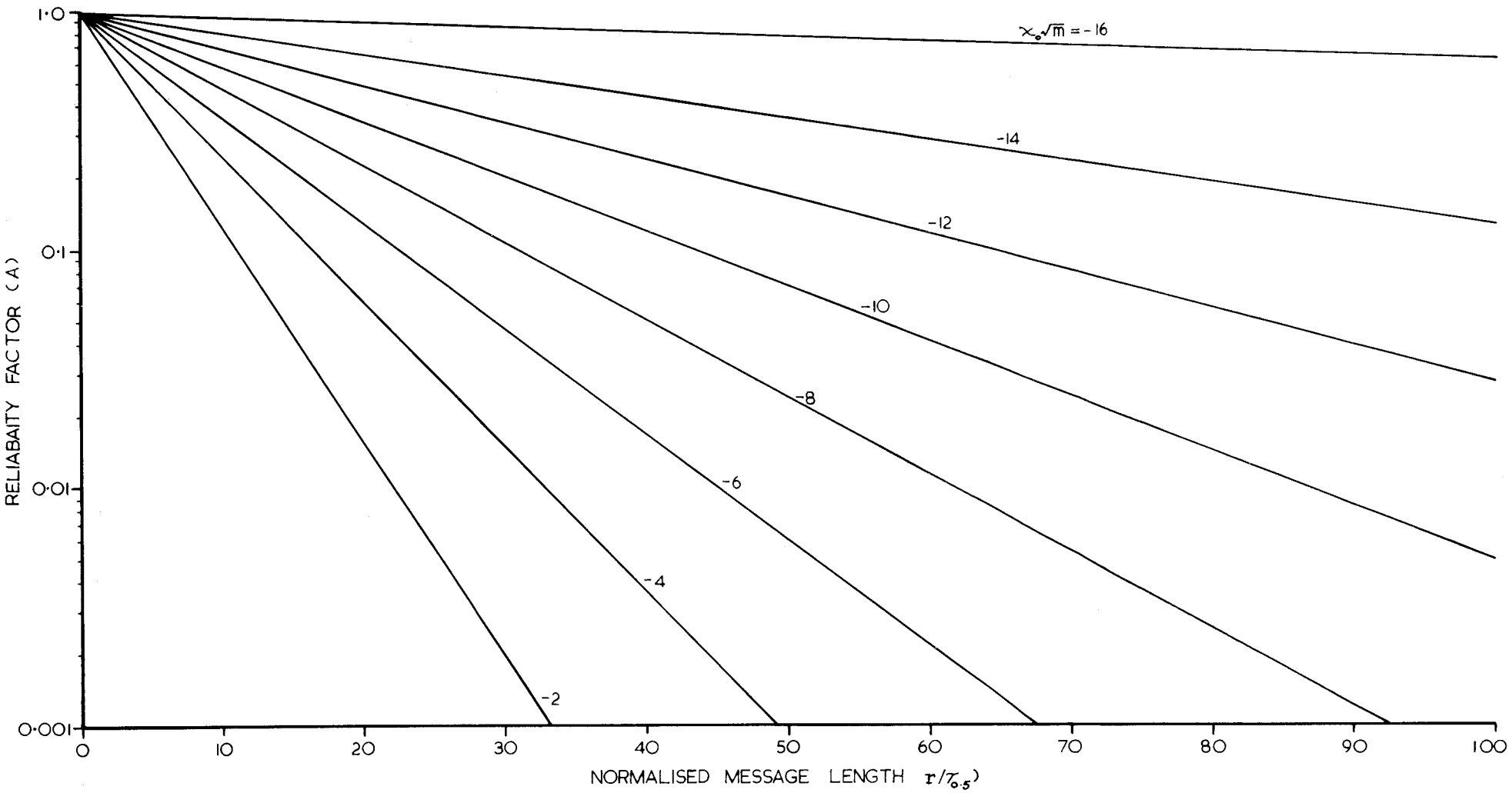

Figure 13. The reliability factor (A) as a function of normalised message length $(r/\tau_{0.5})$ for several values of $\chi_0\sqrt{m}$

DOCUMENT CONTROL DATA SHEET

Security classification of this page: UNCLASSIFIED

1 DOCUMENT NUMBERS

AR Number: AR-001-658

Report Number: ERL-0074-TR

Other Numbers:

2 SECURITY CLASSIFICATION

a. Complete Document: Unclassified

b. Title in Isolation: Unclassified

c. Summary in Isolation: Unclassified

3 TITLE

THE EFFECT OF SCINTILLATIONS ON TRANSIONOSPHERIC COMMUNICATIONS

4 PERSONAL AUTHOR(S):

D.G. Singleton

5 DOCUMENT DATE:

April 1979

6 6.1 TOTAL NUMBER OF PAGES 32

6.2 NUMBER OF REFERENCES: 18

7 7.1 CORPORATE AUTHOR(S):

Electronics Research Laboratory

7.2 DOCUMENT SERIES AND NUMBER

Electronics Research Laboratory 0074-TR

8 REFERENCE NUMBERS

a. Task: DST 76/10

b. Sponsoring Agency:

9 COST CODE:

310876/122

10 IMPRINT (Publishing organisation)

Defence Research Centre Salisbury

11 COMPUTER PROGRAM(S) (Title(s) and language(s))

12 RELEASE LIMITATIONS (of the document):

Approved for Public Release

12.0	OVERSEAS	NO		P.R.	1	A		B		C		D		E	

Security classification of this page: UNCLASSIFIED

Security classification of this page: UNCLASSIFIED

13 ANNOUNCEMENT LIMITATIONS (of the information on these pages):

No Limitation

14 DESCRIPTORS:

a. EJC Thesaurus Terms

Ionosphere
Ionospheric propagation
Spacecraft communication
Scintillation
Communication satellites
Active communication satellites
Radio transmission
Scatter propagation
Ionospherics

b. Non-Thesaurus Terms

15 COSATI CODES:

2014

16 LIBRARY LOCATION CODES (for libraries listed in the distribution):

AACA SR SD SW

17 SUMMARY OR ABSTRACT:
(if this is security classified, the announcement of this report will be similarly classified)

Consideration is given to the bearing ionospheric scintillation has on the design and on the evaluation of the performance of satellite communication links. Emphasis is placed on establishing a design parameter of universal application. The cumulative amplitude distribution function (cdf), which has found application in this regard, is shown experimentally to be well represented by the Nakagami m-distribution at all scintillation levels. However, the cdf is demonstrated to be strictly valid only for amplitude modulated signals of short duration. Auto-correlation, power spectra and level crossing techniques are investigated in an effort to establish a design parameter more universally applicable than the cdf. A quantity message reliability, is defined which removes the short duration restriction inherent in the cdf. A formula for message reliability is developed which allows it to be evaluated for any fade margin and message length, given the scintillation index and the half width of the autocorrelogram of the scintillating channel. A design chart, embodying this information, is also illustrated.

Security classification of this page: UNCLASSIFIED